Sedimentologika

Research article

Multiproxy synthesis at the Arlington Archosaur Site: New insights into Cretaceous paralic paleoenvironments and regional stratigraphy, Woodbine Group, Texas, USA

Christopher R. Noto[1*], Peter P. Flaig[2], Maria Antonieta Lorente[3]

[1] Department of Biological Sciences, University of Wisconsin–Parkside, 900 Wood Rd PO Box 2000, Kenosha, Wisconsin 53141, U.S.A.
[2] Bureau of Economic Geology, Jackson School of Geosciences, University of Texas at Austin, 10100 Burnet Rd., Bldg. 130, Austin, Texas 78758-4445, U.S.A.
[3] Geology, Central University Venezuela and Ellington Geological Services, 1414 Lumpkin Rd., Houston, Texas 77043, U.S.A.

*corresponding author: Christopher R. Noto (noto@uwp.edu)

doi: 10.57035/journals/sdk.2025.e31.1435

Editors: Murray Gingras and Or M. Bialik
Reviewers: Two anonymous reviewers
Copyediting, layout and production: Romain Vaucher and Madeleine Vickers

Submitted: 12.01.2024
Accepted: 24.10.2024
Published: 06.01.2025

Abstract | Ecosystems of the 'mid' Cretaceous are significant but poorly understood, due in large part to a sparse fossil record. Existing fossils, particularly in North America, are not chronostratigraphically well-constrained, further hampering comparisons of species and ecosystems across Laramidia and Appalachia. Efforts to overcome this lack of temporal resolution typically involve systematic collection of ashfall deposits, geochemistry, and biostratigraphy. Here we describe a new, high-resolution palynological and sedimentologic dataset from the Arlington Archosaur Site (AAS) of the Lewisville Formation (Woodbine Group; Middle Cenomanian). The integration of these new data with existing biostratigraphic, macrofossil (vertebrate, invertebrate, botanical), lithologic, ichnologic, and geochemical data allows for a comprehensive paleoenvironmental reconstruction and assessment of paleoenvironmental evolution during AAS deposition. Depositional environments are paralic and include nearshore, shallow-marine tidal-flat, lagoonal, tidal-delta deposits, fluvial-distributary channels, and associated floodplain environments including wetlands (swamp-marsh-lakes) and paleosols. The presence of the *Cyclonephelium compactum – C. membraniphorum* (Ccm) morphological plexus throughout the AAS deposit suggests a younger minimum age of (early) late Cenomanian for deposits, indicating possible southward expansion of this group into the Cretaceous Western Interior Seaway (CWIS) coincident with the onset of the Plenus Cold Event (PCE) of OAE2. The revised age estimate for the AAS suggests that Woodbine deposition at more proximal clastic source areas continued into the late Cenomanian, coeval with down dip Eagle Ford Group sedimentation. This study has important implications for the biogeography of western Appalachia and the response of terrestrial and shallow marine ecosystems of the southeastern CWIS to the onset of OAE2.

Lay summary | The Woodbine Group is exposed between the cities of Dallas and Fort Worth in Texas and preserves a rare set of transitional continental-terrestrial to shallow-marine environments from a poorly known interval during the Late Cretaceous period. Here we describe a newly collected set of fossil pollen, spore, and marine microfossils from a prominent Woodbine locality called the Arlington Archosaur Site (AAS). These specimens, combined with sedimentology provide a highly-detailed record of ecological conditions during AAS deposition, documenting important environmental and climatic changes. Data support previous reconstructions indicating warm and humid, tropical-like conditions while revealing short-term sea-level fluctuations and relative temperature/humidity dynamics not evident in the rocks themselves. Results suggest that the AAS is younger than presented in previous reconstructions, and may correspond to the onset of a globally-recognized oceanic anoxic event called OAE2. A younger age for the Woodbine Group changes how we interpret the fossil plants and animals with respect to regional relationships, and how we compare them to global datasets.

Keywords: Cenomanian; Eagle Ford; Plenus Cold Event; OAE2; Tidal Coastline

This is an open access article under the terms of the Creative Commons Attribution License (CC-BY) © 2025 The Authors

1. Introduction

The transition from the Early to the Late Cretaceous (Aptian to Cenomanian) was a period of major turnover in terrestrial ecosystems, from taxa that typify older Jurassic-Early Cretaceous communities to those which come to dominate the landscape in the Late Cretaceous and form the basis of "modern" communities (Jacobs & Winkler, 1998; Benson et al., 2013; Zanno & Makovicky 2013; Nesbitt et al., 2019; Pérez-García et al., 2020). The global record for this period is relatively poor, especially in North America, which was separated into Laramidia to the west and Appalachia to the east by at least two major marine transgressions resulting in the formation of the Cretaceous Western Interior Seaway (CWIS) (Slattery et al., 2015). Our understanding of this transitional period is largely informed by the more robust Laramidian record, while that of Appalachia remains poor. One important piece of the Appalachia puzzle is found in north-central Texas. The terrestrial rock record of the 'mid' Cretaceous in Texas is fairly extensive, including deposits of the Trinity Group (late Aptian–early Albian), Washita Group (late Albian–early Cenomanian), and Woodbine Group (early–middle Cenomanian). While fossils of the Trinity and Washita Group are well-characterized, the fossil record of the Woodbine Group has received only limited attention.

The Woodbine Group comprises valley-fill, fluviodeltaic, and shallow marine deposits sourced primarily from the Ouachita Mountains of southern Oklahoma and emplaced within the subsiding East Texas Basin and surrounding areas (Dodge, 1952; Oliver, 1971; Trudel, 1994; Ambrose et al., 2009). Previous work described dinosaurs, birds, crocodyliforms, mammals, fish, and invertebrates of the Woodbine Group (Bergquist, 1949; McNulty & Slaughter, 1962; McNulty & Slaughter, 1968; Krause & Baird, 1979; Kennedy & Cobban, 1990; Trudel, 1994; Lee, 1997; Head, 1998; Jacobs & Winkler, 1998; Adams et al., 2011; Tykoski & Fiorillo, 2010; Cavin et al., 2021; Hacker & Shimada, 2021). Though these finds offer some insight into this important fossil assemblage, greater understanding of the biota they represent is hampered by the isolated state of the finds, with many being fragmentary and poorly preserved. The situation improved with the discovery of one particularly productive locality known as the Arlington Archosaur Site (AAS, Figure 1). Detailed surveys and sampling of the site was carried out during several fieldwork campaigns from 2007 to 2017. This work included detailed descriptions of sedimentary characteristics, facies, stratigraphic structure and architecture, and depositional environments (Noto 2015; Adams et al., 2017; Andrzejewski & Tabor, 2020; Noto et al., 2023a) along with characterization of a diverse faunal assemblage (see Main 2013; Main et al., 2014; Adrian et al., 2019, 2021, 2023; Drumheller et al., 2021; Noto et al., 2019, 2022, 2023b; Adams et al., 2023; Ostrowski & Noto, 2023). However, much of this work had yet to be combined in a comprehensive synthesis in order to definitively reconstruct AAS ecosystems and paleoenvironmental evolution.

Woodbine Group exposures in the DFW area generally record marine deposits along a Cretaceous Appalachia tidal coastline that interfinger with more proximal, up-dip coastal plain deposits (Noto et al., 2023a). These types of depositional systems typically contain a lithofacies suite that is notoriously challenging to correlate over even short distances, because the deposits are highly heterolithic and lateral facies changes can occur over 10–20 m. These systems not only exhibit major lateral facies changes, but also contain up-dip and down-dip heterogeneity (e.g., coastal plain to deltaic to tidal shelf facies). Therefore, Woodbine Group outcrops that are correlated using a lithostratigraphic approach may not be correlated chronostratigraphically, resulting in major problems for interpreting the characteristics and evolution of Woodbine deposystems and ecosystems. In addition, palynological studies of the Woodbine Group that can aid in correlations and provide age control are limited, with many describing palynomorphs from localities far from the exposures in the DFW area (Bergquist, 1949; Stephenson, 1952; Hedlund, 1966; Denne et al., 2016).

One way to address this problem is to develop a biostratigraphic, and if possible, sequence stratigraphic framework for the Woodbine Group exposures in the Dallas-Fort Worth area. This would be a major step toward identifying outcrop intervals deposited during the same time period that could be correlated locally. This biostratigraphic framework would improve regional correlations and allow for identification of contemporaneous successions across the CWIS in Laramidia, promoting more accurate comparisons of vertebrate fossil and paleobotanical assemblages. Deposits at the Arlington Archosaur Site present a valuable case study due to a long history of detailed research, high lithologic variability (continental-terrestrial to marine-transitional stratigraphy), potential for high-resolution sampling (cm-scale), and a good preservation potential for palynomorphs. Furthermore, considering the total AAS outcrop thickness is no greater than 2.5 meters, it is extremely difficult to place the sediments into an existing lithostratigraphic framework. It would be much more valuable to employ a multidisciplinary approach in order to provide a high-resolution biostratigraphic framework tied to stratigraphy to refine paleoenvironmental interpretations and provide age control. Therefore, the goals of this study are to: (1) refine the paleoenvironmental interpretation of AAS deposits by combining paleontology, sedimentology, and biostratigraphy, (2) compare these results to previous studies of Woodbine Group palynomorphs, paleoenvironments, and climate proxies, and (3) identify the chronostratigraphic position of the AAS deposits and inclusive biota and point out significant correlations.

2. Characteristics and History of the Woodbine Group

The subsurface characteristics and extent of Woodbine Group deposits have been extensively studied as part of petrochemical development in Texas. The entire Woodbine succession (up to ~330 m) is well documented in abundant drill core and wireline logs (Ambrose et al., 2009; Hentz et al., 2014; Denne et al., 2016). Recent sequence stratigraphic interpretations based on sequence boundaries and flooding surfaces identified the Woodbine Group as a third-order regressive sequence deposited over ~1.5 m.y. (Ambrose et al., 2009; Hentz et al., 2014; Denne et al., 2016). Woodbine fluvio-deltaic deposits vary spatially and temporally (Ambrose et al., 2009; Hentz et al., 2014) with different deposystems occupying different levels in the stratigraphy, reflecting eustatic fluctuations. Ambrose et al. (2009) identified deposits of lowstand, transgressive, and highstand systems tracts. For example, valley incision (sequence boundaries) and valley fill sequences occurred during and immediately following lowstands whereas thick deltaic deposits are deposited during transgressions and highstands. Variable accommodation in the Woodbine was also affected by salt tectonics (Ambrose et al., 2009; Hentz et al., 2014).

Surface exposures of the Woodbine Group form a narrow, irregular band up to 32 km wide and 100 m thick, stretching from central Texas northward into southern Oklahoma (Dodge, 1969; Oliver, 1971; Johnson, 1974; Trudel, 1994). Woodbine Group surface exposures, particularly in the DFW area (Figure 1), include multiple subdivisions that have undergone numerous revisions, with the number and composition of subunits varying with location and investigation (Denne et al., 2016 and references therein). In the study area, current stratigraphic relationships indicate that the Woodbine Group unconformably overlies the Grayson Marl (Washita Group, Figure 1) and is overlain by deposits of the Eagle Ford Group (Oliver, 1971; Johnson, 1974; Ambrose et al., 2009). The Woodbine Group is divided into the lower Dexter sand comprising deposits of marginal-marine and fully marine depositional systems, and the Lewisville Formation, comprising distal coastal plain deposits (Bergquist, 1949; Dodge, 1952; Dodge, 1968; Dodge, 1969; Johnson, 1974; Oliver, 1971; Powell, 1968; Ambrose et al., 2009). Identification of these units in outcrop is based primarily on facies characteristics; however, Woodbine Group subunits can be difficult to identify in well logs (Hentz et al., 2014). The AAS examined here is typically placed within the lower to middle Lewisville Formation based primarily on lithostratigraphic similarity to deposits of that subunit, and the presence of gastropod specimens referable to *Anchura* and *Gyrodes* (Stephenson, 1952).

The age of the Woodbine Group and its internal divisions is debated, in part due to different workers utilizing different primary sources (surface exposure vs. subsurface cores) and a variety of methodologies (lithostratigraphy, biostratigraphy, sequence stratigraphy). Based on sequence stratigraphic and chronostratigraphic data deposition of the Woodbine Group began in the middle-early Cenomanian (Ambrose et al., 2009; Adams & Carr, 2010; Donovan et al., 2016; Vallabhaneni et al., 2016). At least some portion of the early Cenomanian is missing from terrestrial deposits (Jacobs & Winkler, 1998). Age estimates for Cretaceous strata deposited along the CWIS typically rely heavily on marine invertebrate biostratigraphic zones, requiring precise correlation with biostratigraphy of terrestrial units in order to be useful (Jacobs & Winkler, 1998). Consequently, because Woodbine deposits are transitional shallow-marine to continental-terrestrial there is little direct data (marine invertebrates, etc.) for estimating the age of most intervals, and data points are often small, isolated outcrops that are difficult to correlate. Lee (1997) identified the ammonite *Conlinoceras tarrentense* from an outcrop in Bear Creek near the Dallas Fort Worth airport assigned to the Lewisville Formation, providing a minimum age for the Woodbine of early middle Cenomanian (approximately 95-96 MY) (Stephenson, 1952; Kennedy & Cobban, 1990; Hentz et al., 2014; Denne et al., 2016). However, conflicting evidence suggests that some portions of the Lewisville Formation may be as young as late Cenomanian-early Turonian (Christopher, 1982; Kennedy & Cobban, 1990; Jacobs et al., 2005; Ambrose et al., 2009; Cloos, 2018). The Lewisville Formation (Figure 1) is typically identified at the surface based on lithostratigraphy, primarily by relatively high mud/silt content and relatively low sandstone content. However, other intervals of the Woodbine, including parts of the underlying Dexter Formation can have similar lithostratigraphic characters, and are not chronostratigraphically Lewisville equivalent, (Ambrose et al., 2009; Denne et al., 2016). Regardless of the actual age(s) of these deposits, examples such as these serve to illustrate the problems with using lithostratigraphic criteria to correlate and/or assign ages to limited and isolated outcrop exposures of complex, continental-terrestrial to shallow-marine deposystems.

With respect to biostratigraphy, Hedlund (1966) was the first to document the fossil pollen assemblages of the Red Branch Member of the Woodbine in Oklahoma, located stratigraphically near the base of the Lewisville Formation (Bergquist, 1949; Stephenson, 1952; Denne et al., 2016). Hedlund (1966) identified 75 palynomorphs, divided into five assemblages dominated by pteridophytes and angiosperms, and interpreted species as those from a wet, tropical climate regime. Palynomorphs have rarely been used for Woodbine Group biostratigraphic correlation, despite being widespread. For example, the Tarrant Member was moved from the overlying Eagle Ford Group to the Lewisville Formation of the Woodbine Group based, in part, on the similarity with Woodbine palynomorph assemblages (Stephenson, 1952; Brown & Pierce, 1962; Christopher, 1982; Denne et al., 2016). However, many palynomorphs are those of long-lived taxonomic groups of little biostratigraphic value. Christopher (1982) used the presence of *Complexiopollis* and the absence of *Atlantopollis* to identify a temporal relationship between the Arlington Formation and Lewisville Formation, supporting the placement of the Arlington as a member within the Lewisville Formation (Denne et al., 2016). More recently Cloos (2018) sampled three separate Woodbine Group localities along a north-south transect, finding a substantial overlap of palynomorph groups between each

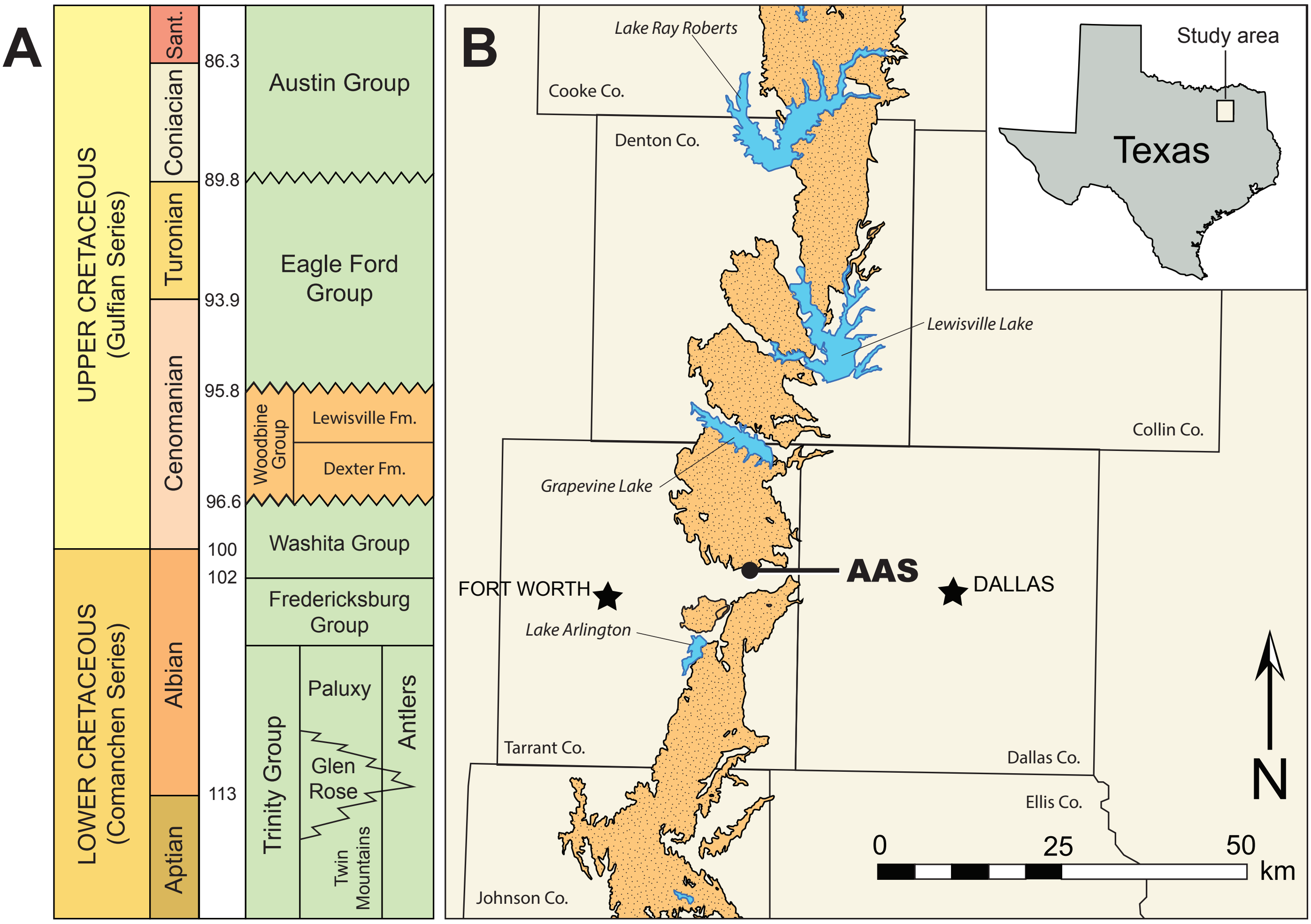

Figure 1 | Location and stratigraphic position of the Woodbine Group in north central Texas. (A) General stratigraphic column and timescale for the Cretaceous. Time scale based on Gradstein et al. (2012) and Denne et al. (2016). Modified from Adams et al. (2011). (B) Map showing Woodbine Group surface exposures in orange including the location of the Arlington Archosaur Site (AAS). Water bodies are blue.

site, particularly the Cuppressaceae, cycads, ferns, and some angiosperms, which thrived under a hot, humid subtropical to tropical climate (Cloos, 2018). An important finding documents the first occurrence of triporate pollen of a Normapolles affinity (?*Pseudoplicapollis* sp.), previously unknown from the Woodbine Group (Cloos, 2018). *Pseudoplicapollis* first appears in the early to middle Turonian, which should indicate a younger age than is currently understood for Woodbine Group deposits in general (Christopher, 1979).

3. Material and methods

3.1. Study area and sampling methodology

The AAS outcrop consists of an approximately 200 m long and 5 m-thick outcrop belt, with the greatest fossil concentrations found in a main quarry that is 2.5 m thick and about 50 m long (Figure 2). Strata dip at approximately 5° to the east. Standard sedimentological techniques were used to describe the quarry deposits (Figure 3). A DJI Mavic 2 pro drone with a 20-megapixel Hasselblad camera was used to capture outcrop imagery. Drone imagery was imported into Agisoft Metashape software, developed into 3D models, and exported as orthomosaics (Figure 2).

A 70 m long section of the outcrop was chosen for palynological sampling including the area where most macrofossils have been recovered. The location of each profile was selected to maximize the vertical extent of facies exposure and/or clarity of borders between facies (Figure 4). The relative position of each section was marked according to a meter-square grid system used for recording the location of fossils uncovered in the quarry, which is anchored by a permanent, georeferenced origin stake. GPS coordinates for each section were also recorded using a handheld Garmin GPS unit. A total of 31 samples of 15-20 g each were collected from fresh surface exposures at different heights measured from the base of the exposure to capture all facies and facies changes in the outcrop (Figure 3). Because of the structural dip of bedding in the outcrop belt, samples taken from the same measured height from base along the strike of the outcrop may not correspond to the same facies association, however facies association changes were noted during sample collection and samples were placed into the corresponding association, and stratigraphic height above AAS base (Figures 3 and 4). The location of each sampled section is shown in Figures 2 and 4.

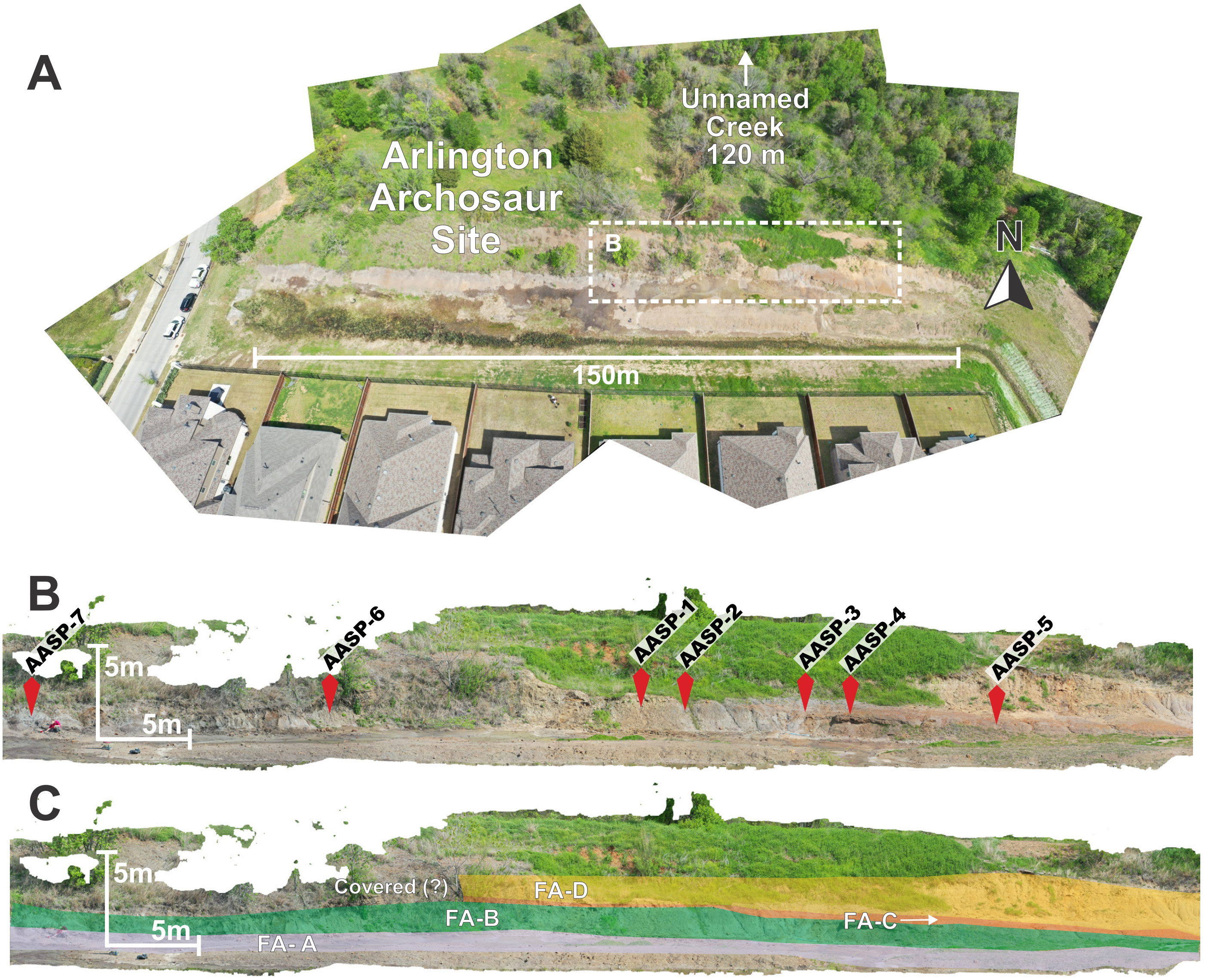

Figure 2 | Overview of sedimentary exposures at the Arlington Archosaur Site. (A) Overhead composite drone image of the entire exposure with inset showing location of sampled sections in B. (B) Ground-level view of exposures, looking north, with the location of stratigraphic columns sampled for palynological analysis. (C) Interpretation of facies association distribution and extent across the sampled portion of the outcrop belt.

3.2. Palynological sample preparation and analysis

We applied a traditional acid preparation technique for this study, e.g., hydrochloric acid (10% HCl) and hydrofluoric acid (70% HF) maceration, then centrifugation in a heavy liquid ($ZnBr_2 \cdot H_2O$), and oxidizing of the organic residue using 10% solution of NH_4OH as needed. We used this technique because samples were indurated, and most studies from similar time intervals used it. A complete description of sample preparation and analysis is provided in Supplement 1. We did this to ensure that the assemblages recovered from the AAS section are comparable with assemblages from similar stratigraphic intervals analyzed by others. Data for select taxa discussed here are available in Supplement 2. The original palynological dataset and detailed results are available in Lorente et al. (2023).

4. Results

4.1. Sedimentology

Four Facies Associations (FA A-D) are described and interpreted for the AAS quarry along with two previously undescribed intervals located below and above the quarry succession (Table 1). The stratigraphic column of the AAS outcrop succession highlights FA characteristics, FA stacking, inclusions, flora, fauna, and interpreted paleoenvironments at the quarry (Figure 3).

4.1.1. Facies Association BQ (FA-BQ)

Located stratigraphically below the AAS quarry, FA-BQ are deposits previously described but currently covered by modern development along with equivalent strata exposed in an unnamed creek located ~120 m north of the quarry (Figures 3 and 5). Facies, trace fossils, and stratal architectures of the sand-rich and heterolithic intervals (Table Facies Associations) are interpreted to record

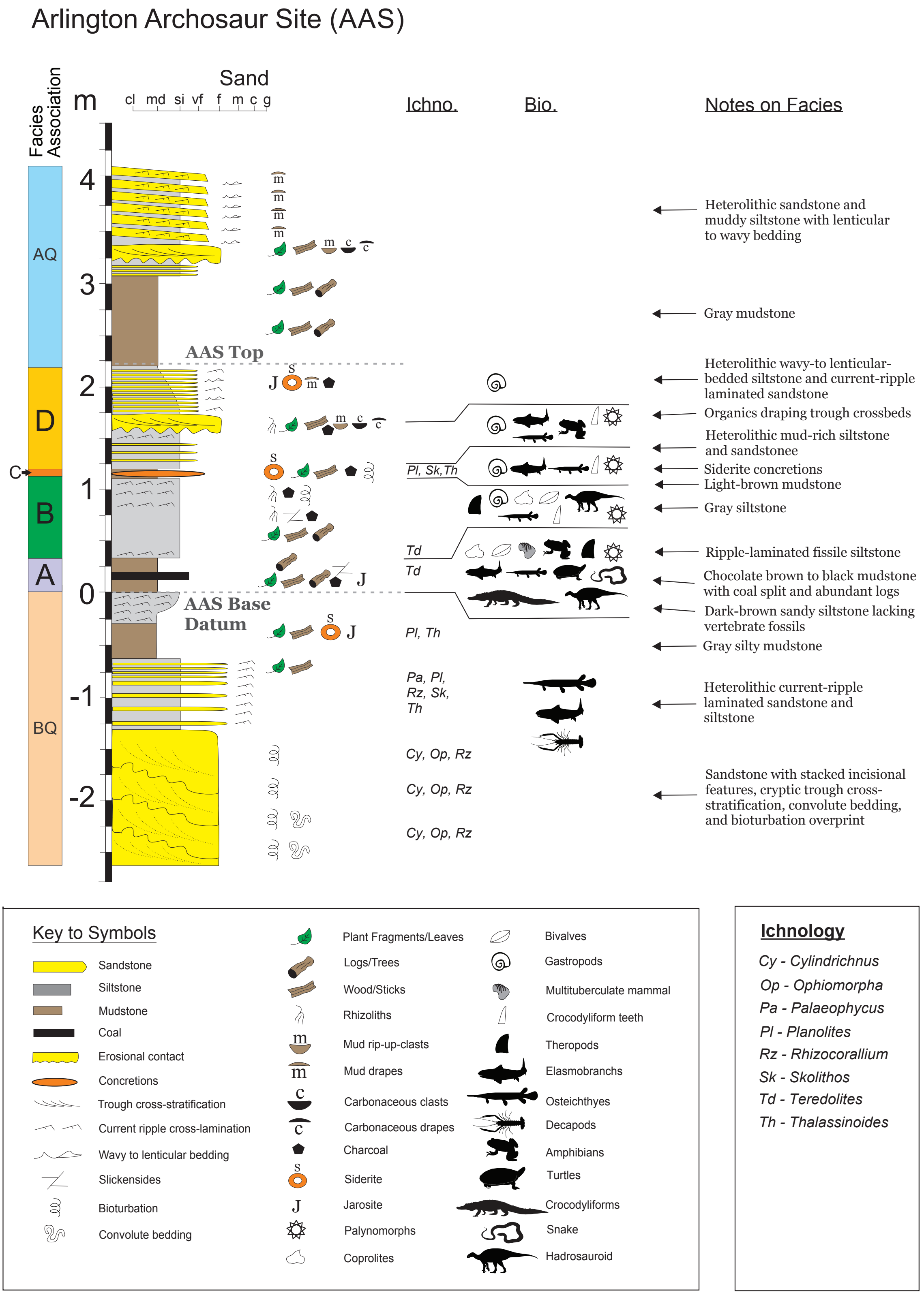

Figure 3 | Stratigraphic section for the Arlington Archosaur Site including fossil distribution, trace fossils, inclusions, and facies association descriptions.

deposits of subaqueous terminal distributary channels or tidal channels along a subaqueous delta front (Buatois et al., 2005; Olariu et al., 2005, Olariu and Bhattacharya, 2006; MacEachern & Bann, 2008; Flaig et al., 2019). The finest-grained deposits represent shallow-marine to continental-terrestrial transitional environments off-axis of the channels or deltas along the distal coastal plain (e.g., Flaig et al., 2011; van der Kolk et al., 2015).

4.1.2. Facies Association A (FA-A)

FA-A are the first deposits considered to be within the AAS quarry above the base datum, and form the primary fossil quarry containing the majority of specimens recovered (Figure 3, Table 1). FA-A preserves abundant plant material, including broad lenticular mats of featureless coalified remains, 15-20 cm wide compressed but well-preserved coalified trees, and permineralized wood (Main, 2013). A large conglomeration of over 20 coalified

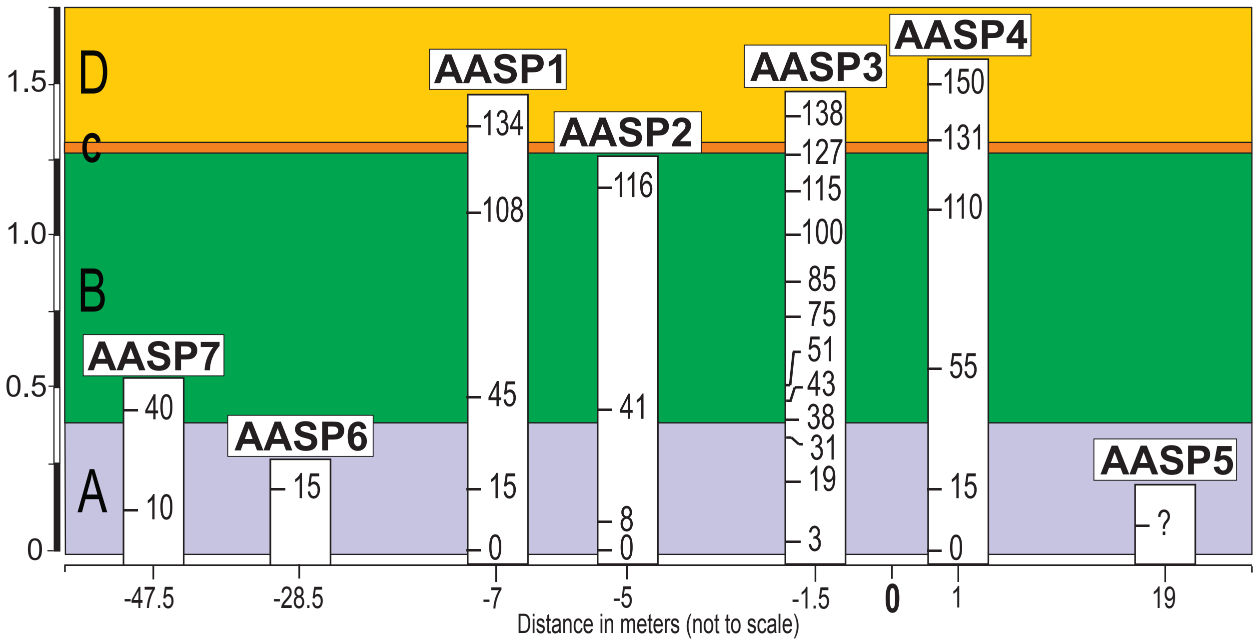

Figure 4 | Simplified stratigraphic section showing locations of sampled columns and distribution of samples within facies associations. Numbers within each column denote height of sample above base datum in centimeters. Lateral distance between sampled columns is measured from georeferenced origin stake in meters (not to scale).

tree trunks 0.5–4.0 m long is found near the base of FA-A (Figure 6). Aligned in a NE-SW direction, these trunks likely represent transported and redeposited wood (Main, 2013). Several well-preserved fern megaspores were also identified (Figure 6). *Teredolites*, a burrow attributed to wood-boring clams that thrive in waters of brackish to fully marine salinities (Buntin et al., 2022), are associated with the transported wood (Figure 6). The presence of *Teredolities* in isolated, transported wood indicates proximity to brackish or fully marine waters (Buntin et al., 2022). FA-A records a transition from the underlying shallow marine deposits and possible shallow-marine brackishwater lagoonal or swamp deposits into terrestrial sourced deposition along a distal coastal plain wetland in swamp, marsh, lacustrine, paludal, or palustrine environments. A nearby fluvial system that transported sediment, trees, and plants is evident. *Teredolities* bored logs indicate adjacent waters with brackish-to marine salinities containing wood-boring clams (Buntin et al., 2022).

4.1.3. Facies Association B (FA-B)

FA-B comprises sandy siltstone containing abundant carbonaceous rhizoliths (Figure 3, Table 1) including several 20-30 cm wide paleo root systems associated with abundant plant fragments (Figure 6), some of which are encased in siderite concretions (Noto, 2015; Adams et al., 2017). Dinosaur fossils attributed to *Protohadros byrdi* are found in the upper portion of FA-B (Noto et al., 2013; Main et al., 2014). Some bones have oysters attached to the bone surface or are in close proximity to it (Figure 6). FA-B records paleosol development, possibly vertisols, or gleyed entisols or inceptisols, on a distal coastal plain proximal to a fluvial channel with a seasonally-variable water table (Retallack, 2001; Flaig et al., 2013). This interpretation is consistent with prior paleosol analyses (Andrzejewski & Tabor, 2020); however, new evidence of abundant oysters suggests proximity to marine waters and a marine flooding event with a transition to shallow-marine deposition at the top of FA-B.

4.1.4. Facies Association C (FA-C)

FA-C consists of laterally extensive (100 m) siderite-cemented silt nodules and erosionally-based, siderite-cemented sand-rich slabs (Figure 3, Table 1). *Planolites*, *Skolithos*, and *Thalassinoides* are common and penetrate into uppermost FA-B. Rare gastropod and bivalves suggest occupation by brackishwater to marine-salinity tolerant organisms (Buatois et al., 2005; MacEachern & Bann, 2008). FA-C is interpreted as a shallow-marine sandbody, such as a splay-delta overlying a paleosol (FA-B), and the result of a marine flooding surface.

4.1.5. Facies Association D (FA-D)

FA-D is dominated by interbedded, fine-grained sandstone (5-10 cm thick) and siltstone (0.1-0.5 cm thick). The interval also includes an erosionally-based sandstone overlain by a fining-upward succession (Figure 3, Table 1). FA-D is interpreted as a shallow-marine tidal flat or mudflat deposit incised into by a tidal channel with probable associated distributary mouth bar deposits (Fan & Li, 2002; Flaig et al., 2019).

4.1.6. Facies Association AQ (FA-AQ)

Deposits above the AAS quarry top datum (FA-AQ) include mudstone, heterolithic siltstone and sandstone, and an erosionally based trough cross-stratified sandstone capped by heterolithics. This interval is interpreted as distal floodplain deposits, possibly from a lake or

Facies Association Designation	Ichnology	Sedimentary Characteristics	Inclusions and Diagnostic Features	Interpreted Depositional Environment
FA-BQ (Below AAS Quarry)	*Cy, Op, Pa, Pl, Rz, Sk, Th*	Fine-grained tough cross-stratified sandstone overprinted by heavy bioturbation. Heterolithic current-ripple laminated sandstone interbedded with gray siltstone along with gray, silt-rich mudstone and dark brown current-ripple laminated sandy siltstone.	Shark teeth, fish fossils, decapod remains, plant fragments, wood fragments and wood impressions, siderite, jarosite. Incisional features including reactivation surfaces overlain by stacked barforms and heterolithics. Soft sediment deformation.	Proximal tidal delta front to distal delta plain.
FA-A (Base AAS Quarry)	*Td*	Dark brown mudstone, dark gray to black highly carbonaceous mudstone, and coal.	Sulfur, pyrite, gypsum, plant fragments, charcoal, coalified wood, tree trunks, permineralized wood, fern megaspores. Vertebrate and invertebrate remains and coprolites. Rare slickensides.	Transitional shallow-marine and brackish lagoonal to swamp-marsh, lacustrine, paludal, palustrine.
FA-B (AAS Quarry)	*Td*	Blocky gray sandy siltstone and light brown sandy siltstone.	Carbonaceous rhizoliths, charcoal, plant fragments, siderite, clastic dykes. Rare shells of aquatic invertebrates, hadrosaurids, oysters, coprolites. Blocky peds with slickensides.	Paleosols.
FA-C (AAS Quarry)	*Pl, Sk Th*	Siderite-cemented siltstone and sandstone.	Plant fragments, wood fragments, charcoal, siderite. Gastropods, bivalves, vertebrate remains. Massive.	Shallow-marine splay-delta.
FA-D (Top AAS Quarry)	--	Interbedded, fine-grained white sandstone and gray siltstone including trough cross-stratification, current ripple cross-lamination, and wavy-to lenticular bedding.	Plant and wood fragments, charcoal, mud rip-up clasts, carbonaceous rip-up clasts, carbonaceous drapes, mud-drapes, siderite, jarosite. Vertebrate remains. Rare marine invertebrates. Rare rhizoliths.	Tidal flat or mudflat including tidal channel and interbedded mouth bar deposits.
FA-AQ (Above AAS Quarry)	--	Interbedded sandstone and gray mudstone with trough cross-stratification, current-ripple lamination, and wavy to lenticular bedding.	Mud clasts, carbonaceous rip-up clasts, carbonaceous drapes, mud-drapes, plant fragments, wood fragments, wood impressions, rare logs.	Distal floodplain including lake/pond, splay/levee, and distributary channel deposits.

Table 1 | Facies Association Table for strata exposed at and around the Arlington Archosaur Site.

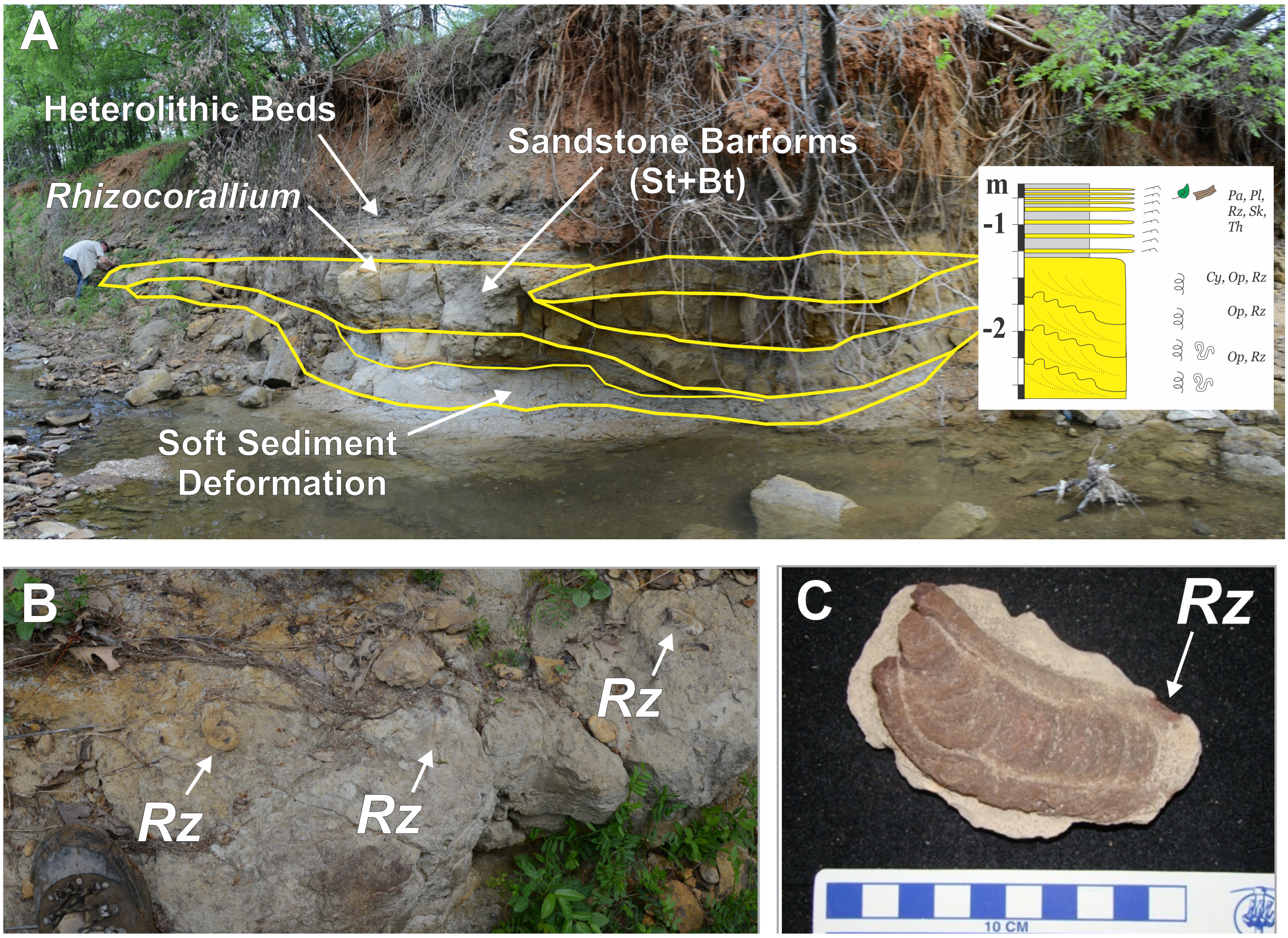

Figure 5 | Exposures in the creek bed north of the AAS outcrop located below the AAS base datum. (A) Interpreted photopanorama of outcrop exposures. Person for scale. (B) Examples of *Rhizocorallium* (Rz) in situ. (C) Collected sample of *Rhizocorallium* from the field south of the AAS quarry.

pond overlain by splay or levee deposits (e.g., Flaig et al., 2011). A distal fluvial-distributary channel with some modification of deposits by tides incises into the underlying deposits (Flaig et al., 2011, 2019, 2022). This uppermost interval records more proximal, coastal plain paleoenvironments compared to the underlying marine deposits of FA-D.

This overall stratigraphic evolution (Figure 3) indicates that paleoenvironments recurrently fluctuated from shallow-marine to continental-terrestrial. It is impossible to deduce from the limited stratigraphy if these fluctuations are related to allogenic (outside of the system) or autogenic (within the system) processes. The AAS succession is progradational overall, from heavily bioturbated shallow-marine sandstone and heterolithics at the base to fluvial-distributary channel and floodplain deposits at the top.

4.2. Vertebrates

The following is a summary of vertebrate fossils and their reconstructed paleoenvironment(s). A detailed listing of currently described taxa, taphonomic disposition, and paleoenvironmental interpretations are included in Table 2. FA-BQ contains vertebrate fossils consistent with nearshore, shallow marine environments, including teeth and vertebrae representing large-, medium-, and small-bodied elasmobranchs and osteichthyans (Main, 2013; Noto, 2015; Ostrowski & Noto, 2017).

Freshwater conditions in FA-A are supported by the presence of salt-intolerant osteichthyans such as lungfish, non-marine turtles, amphibians, and a semiaquatic crocodyliform (Main, 2013; Adams et al., 2017; Drumheller et al., 2021; Adrian et al., 2019, 2021, 2023). Brackish or marine influence is indicated by elasmobranchs and osteichthyans, including individuals a meter or more in length (Noto, 2015; Ostrowski & Noto, 2017). Numerous specimens of dinosaurs, terrestrial turtles, mammals, and non-marine snakes indicate close proximity to land (Ostrowski & Noto 2017, 2023; Adrian et al., 2019; Noto et al., 2019, 2022). These taxa indicate a wetland system along a distal floodplain, proximal to the coastline, with fluctuating freshwater to brackish conditions.

The vertebrate fossils of FA-B belong primarily to a large-bodied (6–7 m length) herbivorous dinosaur that is widely distributed within the Lewisville Formation (Main, 2013; Main et al., 2014; Noto, 2015). Isolated theropod material is also present (Noto et al., 2022). Standing water bodies were nearby on the landscape, evidenced by small elements belonging to teleosts, amphibians, and crocodyliforms. FA-B is interpreted as representing a primarily terrestrial paleoenvironment, such as a delta plain.

Fossils from FA-C are rare and include elasmobranchs and osteichthyans, indicating a return to marine conditions (Main, 2013). Recovery of crocodyliform teeth indicates continued continental influence and/or reworking of terrestrial sediments (possibly from FA-B) during deposition.

Vertebrate fossils known from FA-D are composed of brackish-tolerant elasmobranchs, mixed with freshwater–associated crocodyliform, amphibian, and osteichthyan remains (Main, 2013). This evidence suggests continental-terrestrial distal floodbasin or lagoonal shoreline, with a nearby fluvial distributary channel.

4.3. Palynology

The following palynological associations are used to refine paleoenvironmental interpretations based on lithofacies, ichnology, and paleontology, and limit the age of the exposure. We identified and counted as many terrestrial pollen, spores, algal and fungal remains, and dinoflagellate cysts as possible. Palynological organic matter analysis was out of the scope of this work. Based on the presence of dinoflagellate cysts and the pollen assemblage, both marine and continental-terrestrial deposits are confirmed to be present.

4.3.1. AASP 3-4 section

The assemblage observed in the AASP 3-4 combined column comprises a rich and diversified terrestrial palynoflora and a less diversified, but nonetheless present dinoflagellate cyst assemblage. The terrestrial sporomorph assemblage contains over eighty spore and pollen species, with diversity per sample reaching between 16 and 35 species. These assemblages are characterized by abundant spores, mostly from pteridophytes and pollen from gymnosperms, mostly conifers and, to a lesser extent, angiosperms, although some samples show an increase in angiosperm pollen (Lorente et al., 2023, Figures 4–7). In addition, there is an apparent increase in dicotyledon angiosperm pollen from FA-B up-section. Dinoflagellate cysts are present throughout the column but in lower numbers than sporomorphs, with twenty-four species identified, and a diversity from 1 to 14 species per sample.

A summary of some characteristics observed in the assemblages in the combined section AASP 3-4 (Supplement 2; Lorente et al., 2023 Figure 3, p. 8) include:

- The assemblage richness (abundance and diversity) along the section is highly variable. Still, more than half of the spore species in each sample are from ferns or other seedless plants.

- Pteridophyte (mostly ferns) spores are the most varied single component of the assemblage throughout the section, i.e., various species of *Cyathidites*, *Appendicisporites*, and *Cicatricosisporites,* as well as *Pilosisporites ericius* that is abundant in the lower part of FA-B. Spores from other botanical groups, e.g., lycophytes and bryophytes, are present but scarcer.

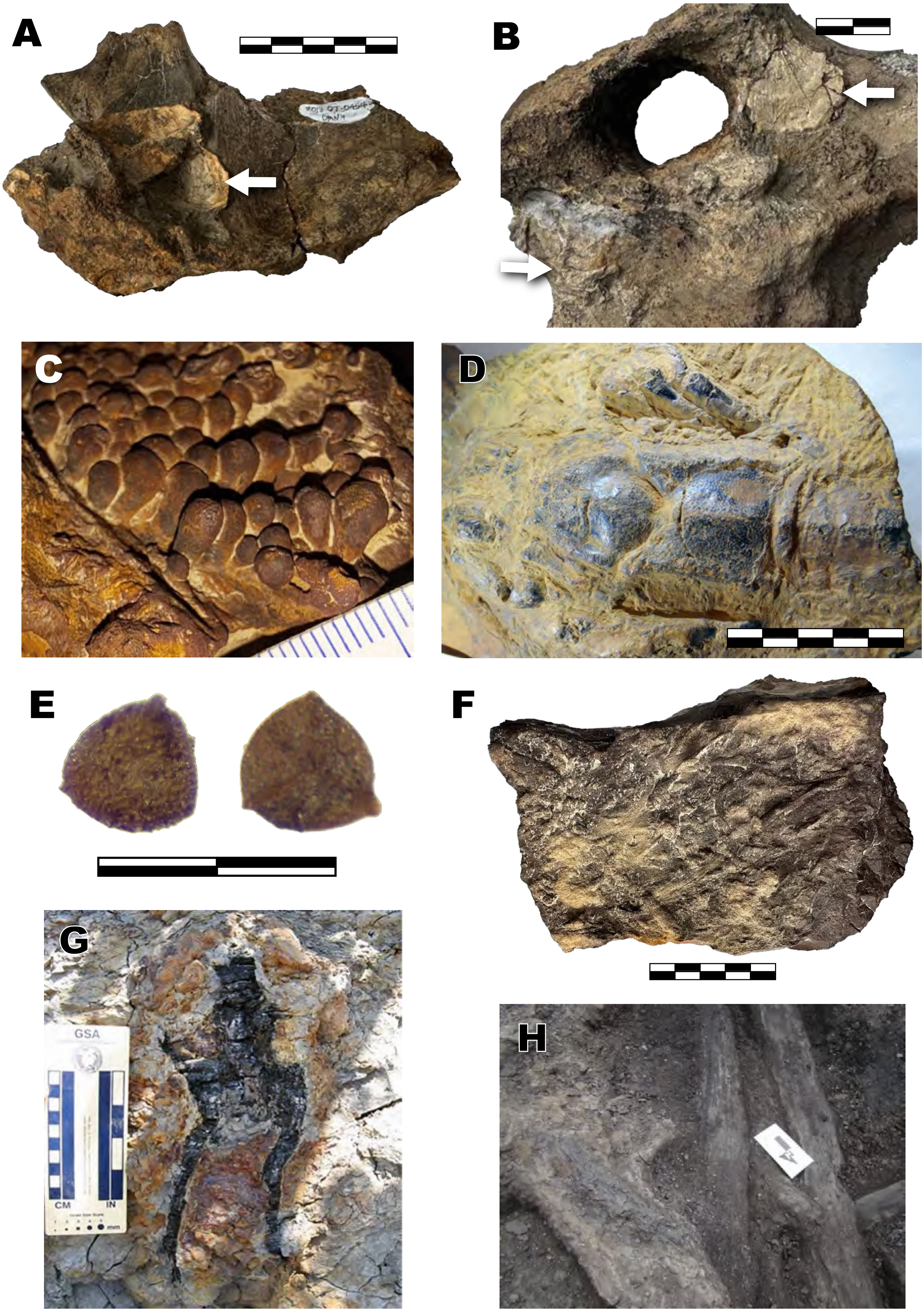

Figure 6 | Sample set of fossils used for indicating paleoenvironmental and depositional conditions. (A) Vertebral arch attributed to the dinosaur *Protohadros* (DMNH 2013-07-0454) with oyster attachment surfaces (white arrow). Scale in centimeters. (B) Dorsal(?) vertebra attributed to *Protohadros* (DMNH 2013-07-0350) with oyster attachment surfaces (white arrows). Scale in centimeters. (C) Infilled burrows of the wood-boring bivalve *Teredolites* in a wood specimen (uncatalogued specimen). Scale in millimeters. (D) Decapod fossil recovered from the creek bed north of the AAS outcrop (uncatalogued specimen). Scale in centimeters. (E) Fern megaspores recovered from sediment screenwashing of FA-A (uncatalogued specimens). Scale bar is 1 millimeter. (F) Invertebrate burrows (DMNH 2013-07-0701) from underlying deposits south of the AAS outcrop (FA-BQ). Scale in centimeters. (G) Charcoalified root system from the upper part of FA-B. Scale bar is 10 centimeters. (H) Multiple carbonized logs found in situ in lower FA-A. Arrow points north and scale is approximately 10 centimeters.

Facies Association Designation	Vertebrate Taxa Identified	Taphonomy	Interpreted Paleoenvironment	References
FA-BQ (Below AAS Quarry)	Elasmobranchs cf. *Cretodus* sp. Odontaspididae indet. *Onchopristis dunklei* Osteichthyes Ichthyodectiform indet. Pycnodont indet. Elopomorpha indet.	Specimens isolated and fragmentary with evidence of modest to high transport. Mix of allochthonous and parautochthonous.	Near shore, shallow marine	Main, 2013; Noto, 2015; Ostrowski & Noto, 2017
FA-A (Base AAS Quarry)	Elasmobranchs Hybodont indet. cf. *Ptychodus* cf. *Pseudohypolophus* Osteichthyes *Enchodus* Pycnodont indet. Ichthyodectiform indet. Amiid indet. Lepisosteid indet. *Ceratodus carteri* Amphibians Caudata indet. Anura indet. Turtles *Gehennachelys maini* *Pleurochayah appalachius* Helochelydridae indet. Trionychidae indet. Protostegidae indet. Crocodyliforms *Deltasuchus motherali* *Woodbinesuchus byersmauricei* *Terminonaris* sp. *Scolomastax salhsteini* *Eusuchia* indet. Crocodyliformes indet. Snake cf. *Coniophis* Dinosaurs Carcharodontosauria indet. Tyrannosauroidea indet. Dromaeosauridae indet. *Protohadros byrdi* Mammals Multituberculate indet. Cladotheria indet.	Skeletal elements well-preserved but disarticulated and isolated (up to 3 m distant); partially articulated specimens rare. Evidence of low-energy, short-distance transport with no clear orientation. Crocodyliform tooth marks on some remains. Autochthonous or parautochthonous.	A transitional shallow-marine to continental-terrestrial deposystem including wetlands along a distal floodplain, proximal to the coastline.	Main, 2013; Main et al., 2014; Noto, 2015; Ostrowski & Noto, 2017, 2023; Adams et al., 2017, 2023; Noto et al., 2019, 2022; Adrian et al., 2019, 2021, 2023; Drumheller et al., 2021; Noto et al., 2023a
FA-B (AAS Quarry)	Osteichthyes Pycnodont indet. Lepisosteid indet. Teleostei indet. Crocodyliform cf. *Deltasuchus motherali* Crocodyliformes indet. Dinosaurs Theropoda indet. *Protohadros byrdi*	Skeletal elements of Protohadros disarticulated but associated; representing dense axial and limb bones. Low to moderate surface weathering. Evidence suggests prolonged subaerial exposure with short-distance hydraulic transport and winnowing. Autochthonous or parautochthonous.	Delta plain with small water bodies	Main, 2013; Main et al., 2014; Noto, 2015; Noto et al., 2013, 2022, 2023b; Noto, 2015; Adams et al., 2023
FA-C (AAS Quarry)	Elasmobranchs cf. *Cretodus* sp. Hybodont indet. Osteichthyes Pycnodont indet. Crocodyliforms Crocodyliformes indet.	Specimens isolated and fragmentary with evidence of modest to high transport. Possible reworking of some elements from lower sediments (FA-B) during deposition. Mix of allochthonous and parautochthonous.	Near shore, shallow marine	Main, 2013; Noto, 2015
FA-D (Top AAS Quarry)	Elasmobranchs Hybodont indet. cf. *Pseudohypolophus* *Onchopristis dunklei* Osteichthyes Teleostei indet. Amphibians Caudata indet. Crocodyliforms Crocodyliformes indet.	Specimens isolated and fragmentary with evidence of modest to high transport. Mix of allochthonous and parautochthonous.	Continental-terrestrial distal floodbasin or lagoonal shoreline with a nearby fluvial distributary channel.	Main, 2013; Noto, 2015
FA-AQ (Above AAS Quarry)	No vertebrate remains have been recovered	No vertebrate remains	No vertebrate remains	

Table 2 | Vertebrate Association Table for strata exposed at and around the Arlington Archosaur Site.

- There are occasional occurrences of gymnosperm pollen, i.e., *Cycadopites* sp. in FA-A; *Rugubivesiculites rugosus* (Supplement 3, Plate 4) in FA-B; and bisaccate pollen from conifers is abundant, especially in the upper part of FA-B and FA-D.

- There are occasional occurrences of angiosperm pollen, i.e., *Aquilapollenites cf. psilatus* (*Aquilapollenites* group) in FA-A, *Aesculiidites dubius* in FA-B, and *Cupuliferoidaepollenites microscabratus* (Supplement 3, Plate 6) that is relatively abundant in uppermost FA-B and throughout FA-D.

- Notable dinoflagellate cyst occurrences are: *Oligosphaeridium pulcherrimum* in FA-A and the lower part of FA-B, two different species of *Florentinia* in lower FA-B are abundant, and the occurrence of *Kiokansium unituberculatum* in the upper part of FA-B. Also relevant is the presence of *Cyclonephelium membraniphorum* (included in the Ccm morphological plexus) throughout the section (Supplement 3, Plate 1). The maximum dinoflagellate cyst diversity reached 14 species at AASP 3-4, 127 cm.

4.3.2. AASP 1-2 section

The assemblage observed in the AASP 1-2 combined column comprises a varied terrestrial sporomorph assemblage and a less diversified dinoflagellate cyst assemblage, similar in proportions to AASP 3-4.

The absolute abundance of specimens per major palynomorph group is variable, with the lower part of FA-A having the most abundant assemblages, although the abundance decreases towards the top of the facies association (Supplement 2). FA-B is moderately rich, and FA-D shows a strong increase in sporomorphs (terrestrial) and a decrease in the abundance of dinoflagellate cysts (marine).

The terrestrial sporomorph assemblage is varied, with over eighty species, including 38 spore species and 42 pollen species (Lorente et al., 2023 Figure 9, p. 12). The spores and pollen assemblages are dominated by spore species of the Cyatheaceae (*Cyathidites* spp.). Conifer pollen is abundant. The angiosperm pollen from *Cupuliferoidaepollenites microscabratus* is abundant at the base of FA-A but not in other facies associations. Cluster analysis of the sporomorph assemblage shows two major clusters: one that includes the samples in FA-A and the lowermost part of FA-B, and a second cluster that includes the samples in the uppermost part of FA-B and FA-D (Lorente et al., 2023, Figures 8 and 9, p. 11 and 12 respectively).

Dinoflagellate cysts are present throughout the section but in lower quantities than sporomorphs. Twenty-six dinoflagellate cyst species were identified, three species of acritarchs, and seven species of freshwater algae, as well as different types of fungal remains (Lorente et al., 2023, Figure 10, p. 13).

A summary of some characteristics observed in the assemblages in the combined section AASP 1-2:

- The assemblage richness (abundance and diversity) along the section is highly variable. Still, more than half of the species in each sample spores are from ferns or other seedless plants.

- Pteridophyte (mostly ferns) spores are the most varied single component of the assemblage throughout the section. Spores from other botanical groups, e.g., lycophytes and bryophytes, are present but scarce.

- Gymnosperms are mainly represented by pollen from conifers, including *Abietineaepollenites* spp.

- Angiosperm pollen of the *Aquilapollenites* group are conspicuous along the section, represented by up to four different species, e.g., *Aquilapollenites cf. psilatus, Aquilapollenites psilatus, Aquilapollenites turbidus,* and *Aquilapollenites* sp. Other angiosperm pollen present includes *Cupuliferoidaepollenites microscabratus,* abundant only in FA-A.

- General assemblage composition and abundance are similar to that observed in the AASP 3-4 combined section.

- There were no Normapolles detected in the section.

- Dinoflagellate cysts from the Ccm morphological plexus are present in FA-A, with most dinoflagellate cyst occurrences restricted to FA-A and FA-B.

4.3.3. AASP 6-7 section

The assemblages observed are less rich in palynomorph species than the ones in combined sections AASP 1-2 and AASP 3-4, mainly due to AASP 6-7 column being restricted to FA-A and lowermost FA-B (Supplement 2).

- There are a total of nine spore species, with the Cyatheaceae (tree fern) spores being largely dominant, including *Cyathidites* spp. and *Cyathidites australis*. Other abundant Pteridophytes spores include *Cicatricosisporites* spp., *Appendicisporites matesovae*, *Concavisporites rugulatus - Gleicheniidites senonicus*,

- There are seventeen pollen species, dominated by the pollen of conifers, which is similar to the assemblages in sections AASP 1-2 and AASP 3-4. Gymnosperm representation is dominated by conifer pollen, including *Rugubivesiculites* cf. *rugosus*, and others like *Cycadopites* sp. / *Ginkgocycadophytus* sp. and *Inaperturopollenites hiatus*.

- Angiosperm pollen is represented by monocots (e.g., palm types) such as *Psilamonocolpites* sp. Other angiosperm pollen is from the *Aquilapollenites* group, including *Aquilapollenites cf. psilatus* and *Aquilapollenites psilatus*. Also present are other miscellaneous pollen types broken or poorly preserved.

In the AASP 6-7 section, the acritarch *Leiosphaeridia* sp. is very abundant, as well as the dinoflagellate cyst *Epelidosphaeridia* cf. *spinosa*, present in lesser amounts are *Cyclonephelium membraniphorum* (Ccm morphological plexus), *Florentinia* cf. *khaldunii*, and miscellaneous dinoflagellate cysts (Lorente et al., 2023, Figure 11, p. 15).

4.3.4. AASP 5 section

Section AASP 5 consists of a single sample collected from FA-A, representing the least diverse and poor assemblage observed in the entire AAS site (Supplement 2). There the sporomorph group is represented by *Cyathidites* spp., *Cyathidites australis*, *Inaperturopollenites hiatus*, and bisaccate pollen (conifers).

The terrestrial sporomorph assemblage has twenty total species (7 spore species and 13 pollen species) which is about a quarter of the richness of assemblages observed in AASP 1-2 and AASP 3-4. The spore assemblage is dominated by species of Cyatheaceae (*Cyathidites* spp.), as in the other sections. Other important and very abundant components of the assemblage are the conifer (gymnosperms) pollen. The pollen from *Inaperturopollenites hiatus* (Taxodiaceae) is more abundant in section AASP 5 than in any other section. The *Leiosphaeridia* sp. acritarch is very abundant. Abundant also is the dinoflagellate cyst *Trithyrodinium* cf. *suspectum* and, in smaller amounts, *Cyclonephelium membraniphorum* (Ccm morphological plexus), *Oligosphaeridium pulcherrimum,* and other miscellaneous dinoflagellate cysts. (Lorente et al., 2023, Figure 12, p. 17). All these characteristics may indicate brackish to shallow marine conditions in FA-A, near the AASP 5 location.

Characteristics of the assemblage in sample AASP 5 can be summarized as follows:

- The assemblages only represent FA-A. The assemblage richness (abundance and diversity) is lower than in AASP 1-2 and AASP 3-4. Still, the most abundant components are spores from ferns or other seedless plants, followed by the pollen of conifers.

- The presence of relatively abundant Taxodiaceae (*Inaperturopollenites hiatus*) pollen, together with a less varied but relatively rich assemblage of dinoflagellate cysts and very low amounts of freshwater algae, distinguish this assemblage from those recorded in AASP 1-2 and AASP 3-4.

- As in the other sections, there were no Normapolles detected.

- Dinoflagellate cysts from the Ccm morphological plexus are present, as well as *Oligosphaeridium pulcherrimum*, *Epelidosphaeridia* cf. *spinosa* and few other dinoflagellate cysts.

5. Discussion

5.1. Sedimentology and paleontology

The sedimentology and ichnology of the AAS site, and the underlying and overlying stratigraphy, provides a basic framework for paleoenvironmental interpretation (Table 1, Figure 3). The vertebrate paleontology provides additional evidence refining the relative influence of marine vs. continental input throughout the AAS section (Table 2). This record indicates fully marine conditions prevailed during deposition of FA-BQ, transitioning to brackish water shallow marine deposits and ultimately to continental-terrestrial distal floodplain wetland deposits in FA-A. Prevalence of a large-bodied dinosaur and limited aquatic taxa in FA-B indicate deposition on a delta plain. FA-C marks the return of near shore, fully marine conditions. The mixture of freshwater and brackish-tolerant taxa in FA-D likely represents a distal floodbasin or lagoonal shoreline with fluvial input. Although robust paleoenvironmental interpretations can be made from the sedimentology, ichnology, and vertebrate paleontology, the palynological data provide the highest-resolution record, which can be used to significantly refine paleoenvironmental interpretations both within and between facies associations.

5.2. Depositional Model for the AAS

The palynomorph assemblage of any sedimentary succession commonly has three main components: *in situ* palynomorphs, redeposited contemporaneous palynomorphs, and reworked palynomorphs from older sediments. Paleoenvironmental interpretation based on palynological results is made by examining the different palynomorph group tendencies in abundance and diversity throughout the section, rather than relying on isolated samples (See Supplement 4, Palynomoprhs as sedimentary particles).

Assuming normal depositional conditions and no significant reworking of older sediments, to determine which components of the assemblage are *in situ* (hence represent a "true" environmental signal) and which elements are transported (representing the signal from the greater drainage basin), the AAS section must be analyzed from a "source to sink" point of view (Figure 7). The source and transfer areas are all locations topographically above the base level, where there is a balance between deposition and erosion (Catuneanu, 2006). The base-level surface is typically either the water table (continental-terrestrial) or the ocean surface (marine).

A model for interpreting the palynological associations found in different depositional paleoenvironments of the AAS site is shown in Figure 8. The diagram illustrates how palynomorphs were dispersed across the topographic profile, from source to sink, i.e., from uplands to the shallow marine shelf or open marine basin. The model only includes palynomorphs found at the AAS site.

Very few samples in the AAS sections represent exclusively terrestrial paleoenvironments since most assemblages bear marine palynomorphs, but it includes some levels that might be tidally influenced. From an abundance-of-specimens point of view, these assemblages are dominated by terrestrial palynomorphs.

Signals observed in the palynomorph assemblage are from at least three parts of the source and transit areas of the source-to-sink system. They are evident in the assemblage (Figures 7 and 8) as follows:

- Sporomorphs in FA-A and lower part of FA-B indicate a vegetation signal from wetlands and swamp forest, based on the abundance and species of pteridophyte spores and conifer pollen, including the presence of Taxodiaceae pollen.
- Sporomorphs and other palynomorphs in FA-B (upper part) indicate a vegetation signal from fluvial bank's forest, ponds or lakes, wetlands, marshes, supported by a strong increase in the amount of fresh water plant spores and algae. A signal from salty swamps is supported by sporadic ocurrences of *Classopollis* spp. (Cheirolepidiaceae) known to inhabit brackish or even hypersaline coastal marshes (Smith et al., 2024).
- Sporomorphs assemblage in FA-D show vegetation signals consistent with upland forests and alluvial-fluvial vegetation based on the abundance of fern spores and gymnosperm pollen. Also significant, is the presence of *Cycadopites* sp., a pollen type associated with cycads which need of beetle pollination (Norstog, 2023) and hence have limited pollen dispersion. Since living cycads inhabit different habitats mainly as components of the forest understory in rainforests and seasonally dry forests, or in "grasslands forming a kind of savanna" (UCMP, n.d.), its pollen may be a signal from widespread tropical lowland(?) seasonal forests, or grasslands nearby the sedimentation locations (sink).

The AAS section show the presence of spores from floating freshwater ferns and angiosperm pollen in assemblages dominated by pteridophyte spores and conifer pollen mixed with a moderately diverse dinoflagellate cyst assemblage. The dinoflagellate cysts are the only elements considered *in situ*, representing paleoenvironments in the sink area, while the rest of the assemblage represents the signal from upland vegetation. These assemblages are common in FA-A and the lower part of FA-B (Figures 7 and 8). A few rich dinoflagellate cyst assemblages are mixed with bisaccate spores and smaller angiosperm grains, suggesting the influence of shallow marine paleoenvironments in some parts of the section, such as in the upper part of FA-B.

5.3. Evidence for shoreline migration over time

The sedimentology, ichnology, and vertebrate paleontology of the study area provide an estimate for millenial scale (10^3–10^5 years) paleoenvironmental changes, however time-averaging masks short-term shifts (decadal-century scale) in shoreline position and depositional environment (marine vs. continental) (Martin 1999; Behrensmeyer et al., 2000). The paleoenvironmental interpretations derived from palynological analysis confirm interpretations derived from sedimentology and paleontology; however higher-resolution palynology (cm-scale) reveals additional shorter-term paleoenvironmental shifts not evident from any other data, providing a fuller picture of the dynamic nature of this ecosystem (Figure 8).

The following assemblages were identified based on the Harris and Tocher (2003) dinoflagellate cyst assemblages related to salinity: Euryhaline assemblages supporting lowered salinities (*Cyclonephelium vannophorum* and *Oligosphaeridium pulcherrimum);* Stenohaline assemblages supporting only normal marine salinities (*Oligosphaeridium totum);* and Offshore assemblages, supporting only normal marine salinities (*Cyclonephelium membraniphorum).* The association found in the AAS section is dominated by euryhaline assemblages with tolerance to salinity changes (See Supplement 4, Paleoecological implications of dinoflagellate cysts), with a lower abundance of stenohaline and offshore types. Major peaks in dinoflagellate cyst diversity are driven primarily by Gonyaulaceans, which increase towards the coastline (shallow marine). Smaller peaks in Peridiniacean diversity, associated with more open marine environments, occur immediately before or after Gonyaulacean peaks. While the signal is primarily shallow marine, these smaller peaks indicate variation in the characteristics of the marine water. The oscillations in shallow marine paleoenvironments in the AAS section may also indicate variations from lower to higher productivity intervals, relative water depth, and the amount of nutrients in the water. Increases in dinoflagellate cysts that prefer offshore settings (colder normal marine water) are evident, e.g., *Cyclonephelium membraniphorum- compactum*, as well as dinoflagellate cysts that thrive in shallow marine waters with decreased salinity, e.g., *Florentinia*, *Hystrichosphaeridium,* and *Oligosphaeridium*.

Dinoflagellate cyst diversity is related to the amount of environmental stress, as environmental stress decreases the richness of the dinoflagellate cyst assemblage

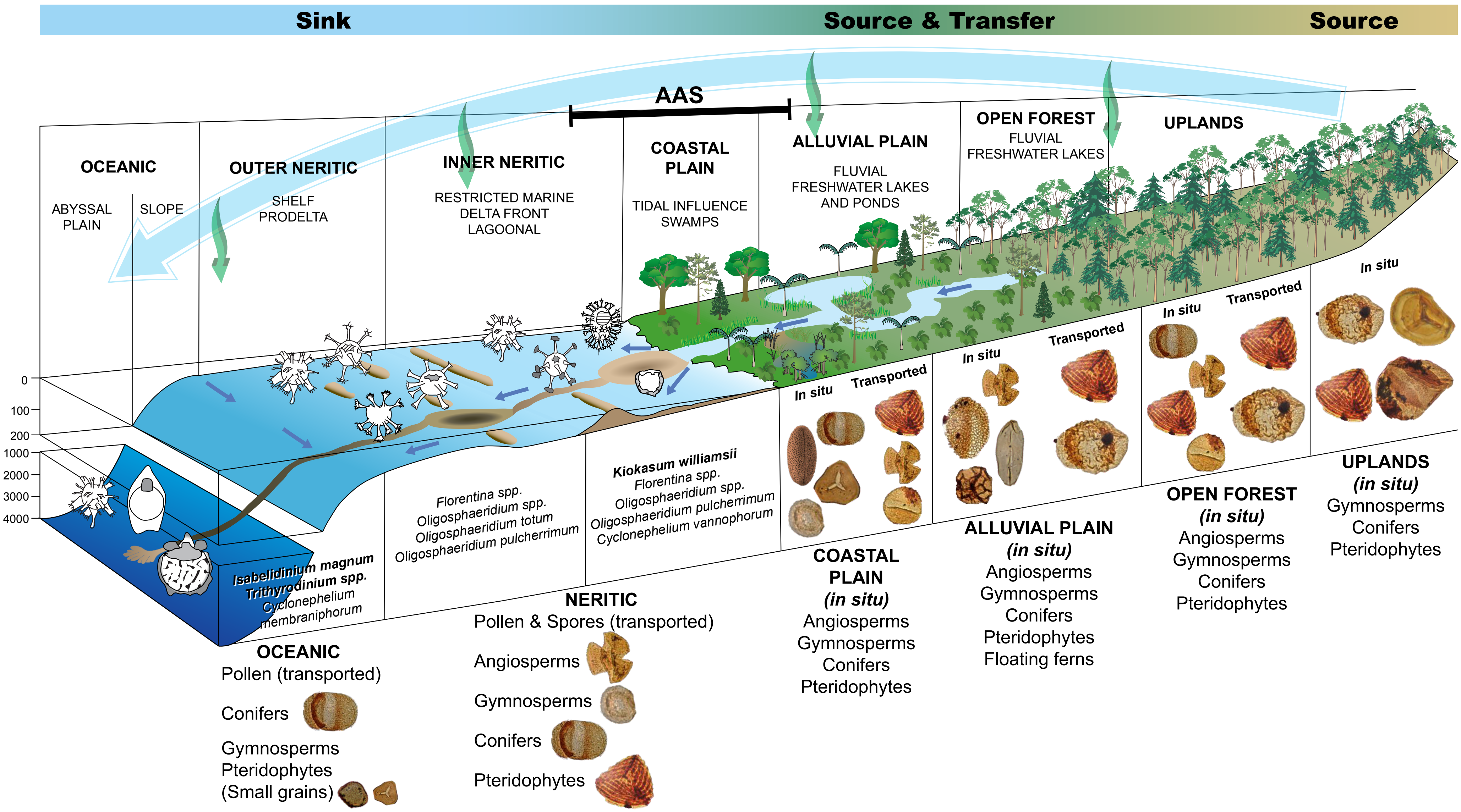

Figure 7 | Idealized model representing the interpretation of paleoenvironments at the AAS in the basin context and the complex dynamic of palynomorph transport and redeposition. The uppermost bar represents an application of the Source to Sink (S2S) Systems model as described in the text. The light blue arrow represents transport by wind, and the smaller green arrows represent the pollen rain. Small dark blue arrows represent transport by currents. In the marine realm, there is the redistribution of dinoflagellate cysts and transported pollen by currents. Sources for this model are the author's own experience and different studies (e.g., Muller, 1959; Williams & Sarjeant, 1967; Tschudy, 1969; Wall et al., 1977; Heusser & Balsam, 1977, 1985; Chowdhury, 1982; Mudie, 1982; Heusser, 1985, 1988; Lorente, 1986, 1990; Farley & Dilcher, 1986; Poumot, 1989; Dupont & Agwu, 1991; Brinkhuis, 1994; Harris & Tocher, 2003; Abbink et al., 2004; Sluijs et al., 2005; Barron, 2015; Heimhofer et al., 2018).

increases from near-shore to distal-offshore environments (e.g., Olde et al., 2015, Dodsworth, 2016). Alternatively, specimen abundance may indicate a bloom of individual species that thrive in specific conditions. We propose that the levels with notable increases in diversity and abundance of the dinoflagellate cyst assemblages (as seen in FA-B) and the presence of representatives of the Ccm plexus (FA-A and uppermost FA-B) record possible (marine) flooding surfaces or marine incursions in relation to a fixed position along the coastline (Figure 8).

5.4. Climate conditions during AAS deposition

The palynological dataset provides further insights into climatic conditions during deposition of the AAS section. The palynology suggests that the climate was cooler and less humid at the start of FA-A sedimentation (Figure 8), with conditions warming towards the top of FA-A, allowing for the development of conifer-forest communities elsewhere in the drainage basin. In the lower part of FA-B, upland pollen is evident, with some conifer-forest coverture, indicating relatively warmer temperatures and higher humidity. Conditions changed in the middle part of FA-B where the warming trend seems to revert to cooler and drier conditions, favoring the growth of open savannah vegetation. From the upper part of FA-B and continuing into FA-D, no clear dominance of any group exists. Still, the presence of a more diversified angiosperm population that included monocots and dicots may indicate cooler and drier conditions, especially towards the top of FA-D compared to the warmer and more humid climate recorded in the uppermost part of FA-A.

The climate changes recorded at the AAS section are of short duration and most are probably driven by obliquity and precession Milankovitch cycles. These results coincide with those from phyllosilicate analyses (Andrzejewski & Tabor, 2020), which provide an estimated temperature of 27±3 °C for in-situ soil phyllosilicate crystallization temperatures for the middle part of FA-B, with air temperatures being probably lower by a couple of °C (25±3 °C) according to authors' estimations. These temperatures, although notably hotter than present day, represent a relative cooling trend from the 31±3°C (or 29± 3°C air temperature) calculated for the Albian-age upper Antlers Formation (Andrzejewski & Tabor, 2020).

The recovered taxa are consistent with the presence of predominantly warm and humid conditions during AAS deposition, further supporting the extension of tropical-like (megathermal) conditions into temperate paleolatitudes under greenhouse conditions that prevailed during the Cretaceous (Noto et al., 2023a).

In addition to previously reported evidence for monsoon-like seasonality, changes in angiosperm and gymnosperm abundance appear to capture Milankovitch-scale changes in relative temperature and humidity during AAS deposition. Furthermore, the cooler and drier conditions observed at the base of FA-A correspond to peak abundance of the Ccm morphological plexus, which here we associate with onset of the Plenus Cold Event (see next section). These associations support the role of a larger-scale mechanism(s), such as Milankovitch cyclicity, driving these changes.

5.5. Refinement of Woodbine Group age and stratigraphic relationships

Woodbine Group strata exposed in the outcrop belt from Grayson to Bell counties, TX, were deposited in the western East Texas Basin, and are separated from coeval subsurface deposits to the east by the Mexia-Talco fault zone (Ambrose et al., 2009). This stratigraphic discontinuity has made outcrop to subsurface correlations challenging, particularly with regard to chronostratigraphy. The minimum age for the Woodbine Group outcrops in the DFW area is largely based on the ammonite *Conlinoceras tarrantense* found in Tarrant County (Lee, 1997). However, the precise stratigraphic relationship of those fossils relative to other exposures in the area is difficult to establish. Also, the morphospecies *Conlinoceras tarrantense* includes other, formerly separate, species mentioned in older literature, e.g., *Calycoceras (Conlinoceras) gilberti*. It is possible that the Tarrant Co. species *C. tarrantense* is found in more than one stratigraphic interval in the Woodbine. *Conlinoceras tarrantense* has an assigned age of 95.73 (±0.61) Ma, according to the revised ammonite zonation and radiometric ages for the CWIS (Cobban et al., 2006). Other authors assign it a slightly younger age of 95.3 Ma (Scott et al., 2004).

Many authors have worked on the complex Cenomanian–Turonian stratigraphy of the CWIS and NE Texas (Sellards et al., 1932; Brown & Pierce, 1962; Christopher, 1982; Dodsworth, 2016; Donovan et al., 2016). Dodsworth and Eldrett (2019) reported on sections of the CWIS related to the consistent FO of *C. membraniphorum* (Ccm Plexus) at higher stratigraphic levels (i.e., intra-Upper Cenomanian) in many mid-latitude sites, such as Pueblo, CO. Also, other locations within the central CWIS (Harris & Tocher, 2003) and Texas (Eldrett et al., 2014, 2015a, 2017) may have evidence of a southerly incursion of a Boreal water mass during the Plenus Cold Event (PCE). The PCE records the temporary interruption of greenhouse conditions during Oceanic Anoxic Event 2 (OAE2) in the latest Cenomanian–earliest Turonian (95–94 Ma), as peak transgression established connections between the CWIS and northern boreal water mass (Eldrett et al., 2017). The *Cyclonephelium compactum – C. membraniphorum* (Ccm) morphological plexus (van Helmond et al., 2016) is listed as one of the dinoflagellate cyst taxa that migrated south during the PCE (Eldrett et al., 2017; Falzoni & Petrizzo 2022). Also relevant is the last occurrence of the dinoflagellate cyst species *Kiokansium unituberculatum* and *Kiokansium williamsi,* which are restricted to the earliest part of the late Cenomanian with an age of ca. 95.6 Ma assumed for both bioevents (Eldrett et al., 2017; Dodsworth & Eldrett 2019).

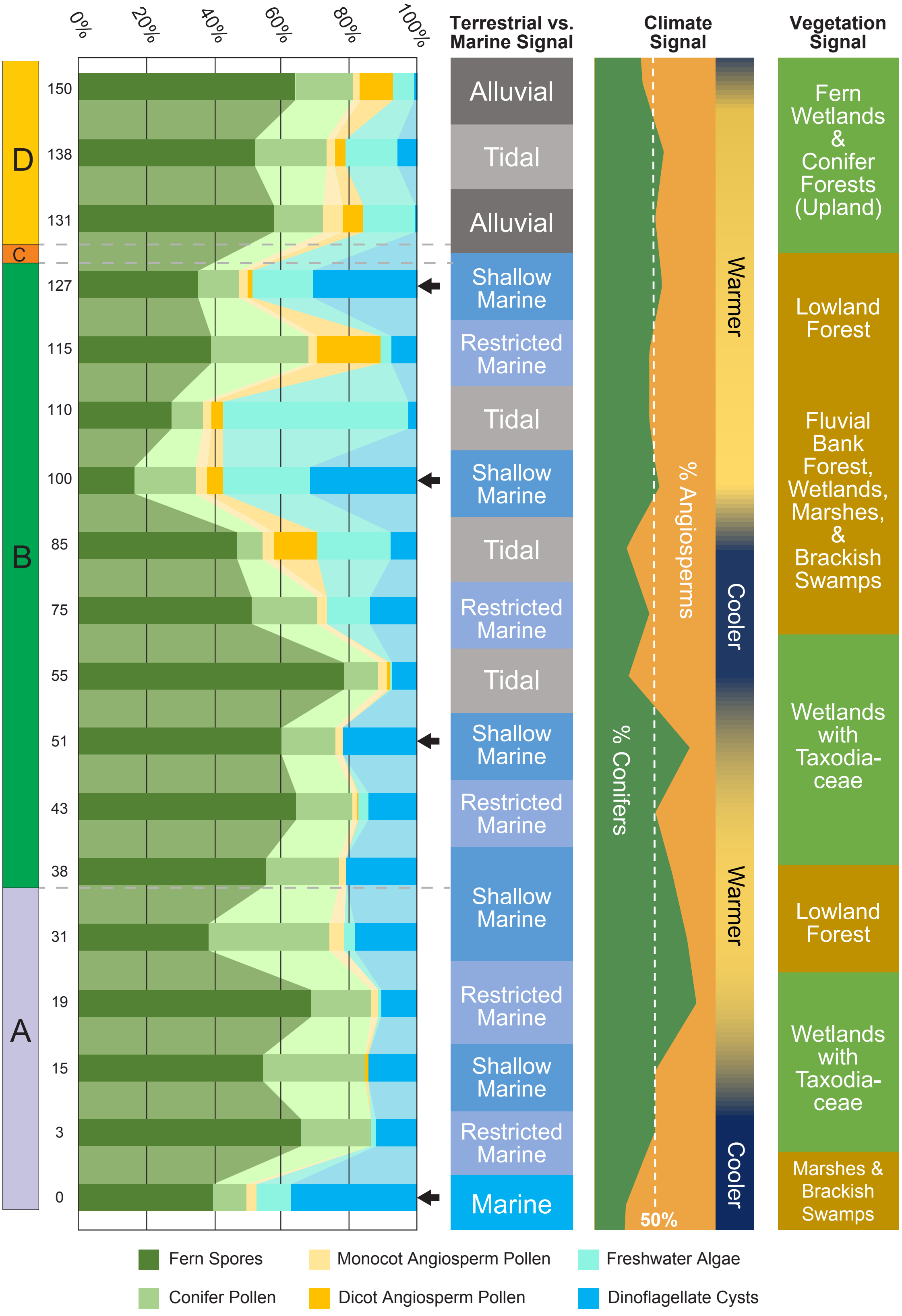

Figure 8 | Combined palynomorph and paleoenvironment chart with the interpretation of signals from the palynological assemblage. The first column, to the left, is the percentage abundance graph of major palynomorph groups (fern spores, conifer pollen, angiosperm (monocot) pollen, angiosperm (dicot) pollen, freshwater algae, and dinoflagellate cysts). Groups are organized according to the main paleoecological preference from "more" terrestrial to marine. The columns to the right of the percentage (%) graph indicate different signals interpreted from the palynomorph assemblages. The column "terrestrial – marine signal" is based on the variation of the percentage of marine dinoflagellates in relation to the total palynomorph assemblage. Based on authors' experience assemblages with over 20% dinoflagellate cysts are considered marine, while assemblages with over 90% terrestrial palynomorphs point to tidal–alluvial conditions, and assemblages with 10% to 19% dinoflagellate cysts are considered shallow to restricted marine. The climate column is based on the percentage relationship between conifers and angiosperm pollen, indicating a change in the composition of the plant communities, with higher percentages of angiosperm pollen related to the proliferation of open, savanna-type vegetation during cooler climate, and a higher percentage of conifer pollen pointing to conifer-dominated forests during warmer conditions (Heimhofer et al., 2018). The final column "vegetation signal" is based on changes in abundance of sporomorph paleoecological associations along the section. The black arrows indicate possible marine flooding events, associated with relevant increases of dinoflagellate cysts in the assemblages.

At the AAS, there are apparent top occurrences of *K. williamsii* (Figure 9) and *Cyclonephelium compactum – membraniphorum* (Ccm Plexus) (Supplement 3, Plate 1), while *K. unituberculatum* (Supplement 3, Plate 3) is present along the entire section (Figure 9). The Ccm Plexus has a continuous presence through the AAS section with a major abundance pick (>11%) at the base of FA-A, with several smaller picks (≥ 6%), indicating the onset of a Boreal water incursion consistent with the PCE (Supplement 4, Figure 1).

The integration of palynological evidence, including the identification of the *N. albertensis* Interval Zone (Lorente et al., 2023), the dinoflagellate cyst *C. membraniphorum* Interval Zone, and the identification of the Ccm morphological plexus in the section that records the possible onset of the PCE, all together suggest a younger age range than is presently reported for the AAS (Figure 9). This supports an age reconstruction for the AAS section as most probably (early) late Cenomanian, in the sense of Ogg and Hinnov (2012).

The revised age estimate for the AAS alters the chronostratigraphic distribution of the Woodbine Group locally, without changing the identity, age, or position of established stratigraphic units in the area. The AAS represents deposits of a unique, up-depositional-dip clastic point source that persisted until the (early) late Cenomanian and was active during deposition of the more distal, down-dip deposits of the Eagle Ford. Our data support previous conclusions based on sequence stratigraphic, lithostratigraphic, and biostratigraphic evidence that some portions of the Woodbine Group may be as young as late Cenomanian-early Turonian, with deposition ending at 92 mya (Christopher, 1982; Kennedy & Cobban, 1990; Jacobs et al., 2005; Ambrose et al., 2009; Cloos, 2018).

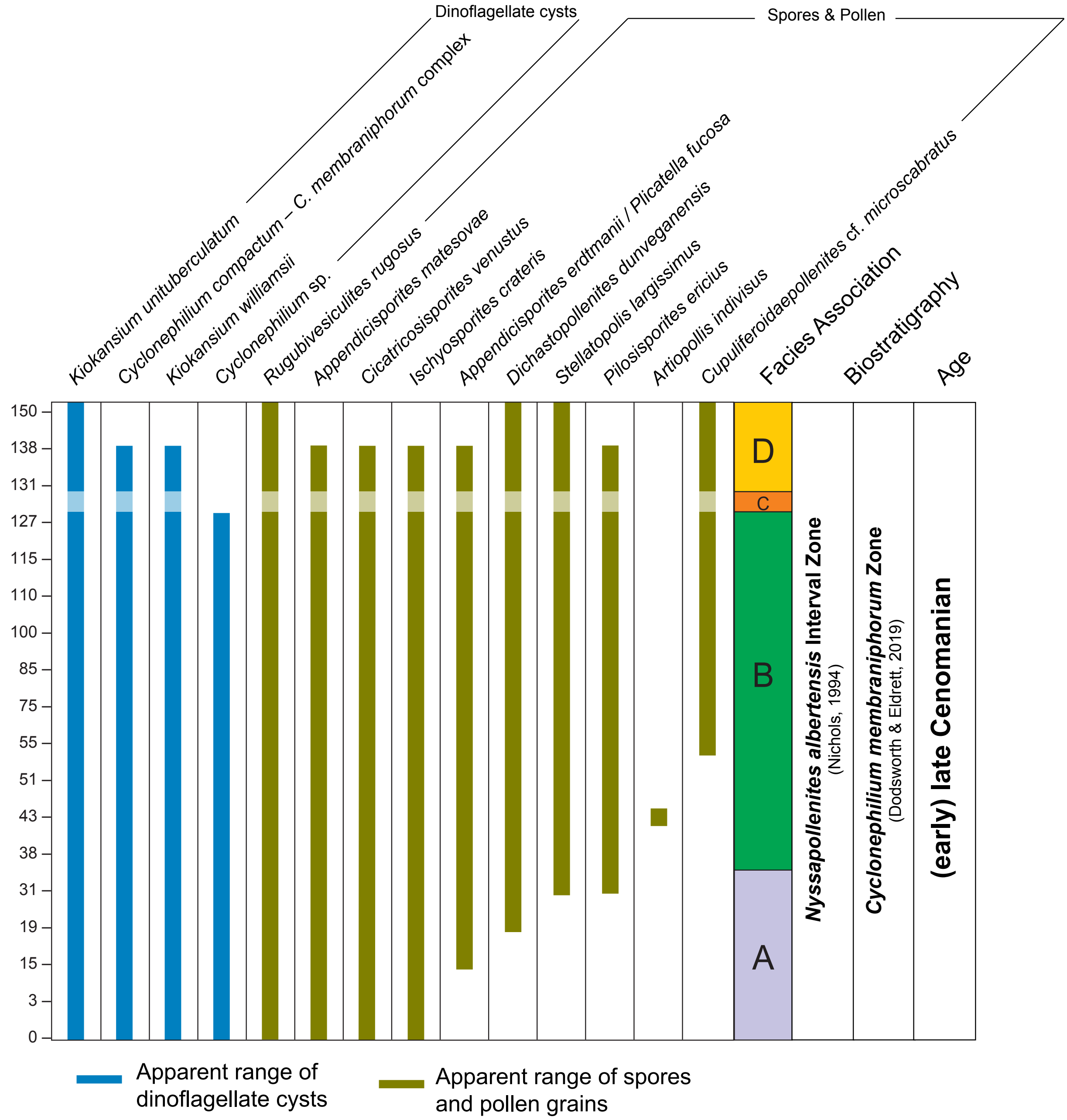

Figure 9 | Range chart showing apparent ranges of key taxa within the combined AASP 3-4 section relevant to the revised age estimation for the exposure. Facies association, biostratigraphic zones, and corresponding age follow to the right. Bars between samples 127 and 131 are transparent since no palynology samples were collected from FA-C.

This extended period of deposition places sediments of the AAS quarry as up-dip, contemporaneous deposits of the (lower) Eagle Ford Group (Denne & Breyer, 2016; Denne et al., 2016; Gifford, 2021). Chronostratigraphically, the AAS deposits should correlate with one of the sandier, less organic-rich intervals of the Eagle Ford stratigraphic "event" that occurred during the (early) late Cenomanian at the onset of the PCE of OAE2.

The potential younger age for the AAS strata has biogeographic implications for the included fossil assemblage. A (early) late Cenomanian age suggests that the AAS could be considered penecontemporaneous to the uppermost Mussentuchit Member of the Cedar Mountain Formation or even the lower Naturita Sandstone (formerly the "Dakota Sands") in Utah (Tucker et al., 2020, 2024), the lowermost Iron Springs Formation (late Cenomanian-Turonian) (Eaton et al., 1997; Eaton, 1999), and the upper Tuscaloosa Group of the Gulf Coastal Plain (Cenomanian-Turonian) (Adams & Carr, 2010). This may also impact other Woodbine Group strata, as the AAS shares multiple taxa (*Protohadros*, *Deltasuchus*, *Terminonaris*, and *Gehennachelys*) with other localities spread across the DFW area, suggesting the existence of a single, coeval fauna (Noto et al., 2022, 2023b; Adrian et al., 2023). However, further chronostratigraphic data from these sites will be necessary to test this hypothesis.

6. Conclusions

The comprehensive synthesis of lithologic, ichnologic, paleontologic, and palynologic data from the Arlington Archosaur Site provides a picture of a biotically diverse, distal coastal plain/delta plain undergoing gradual progradation while experiencing multiple short-term marine incursions. Systematic, fine-scale palynological sampling both supplements paleoenvironmental interpretations based on the lithologic or fossil record and identifies short-term environmental changes not otherwise reflected in those sources. This dataset provides a unique window into a dynamic depositional setting transitional between the continental-terrestrial and marine realms.

The recognition of the Ccm morphological plexus in the AAS section extends deposition into at least the (early) late Cenomanian. This places the outcrop as depositionally contemporaneous with portions of the Eagle Ford Group (Denne & Breyer, 2016). Furthermore, presence of the Ccm morphological plexus confirms the southward expansion of the Plenus Cold Event (PCE) along the CWIS Appalachia coast during the onset of OAE2. If coeval with the dawn of the PCE, the AAS presents valuable insight into the response of terrestrial communities to the onset of OAE2 along the southeastern coast of the CWIS in Appalachia. The dataset establishes the groundwork for comparison with other Woodbine Group surface and subsurface datasets, and those from across the CWIS in Laramidia.

Acknowledgements

The authors would like to thank the Huffines family and Robert Kimball of Viridian Development for granting land access throughout the duration of the AAS project. The specimens described here were made possible by the small army of dedicated volunteers that helped excavate, screenwash sediment, and sift through concentrate for fossils, including community members from Dallas, Fort Worth, and students at UW–Parkside. Special recognition goes to Perot Museum of Nature and Science staff, Ron Tykoski and Karen Morten, for access to AAS specimens and research support. Ron Tykoski generously supplied photos used to create Figure 6. Special thanks to Ellington Geological Services for providing the time and resources to complete this work. National Petrographic helped support this research by providing sample preparation at a reduced price. Nancy Englehart-Moore initiated the original work that directly contributed to this study. We would like to acknowledge two anonymous reviewers, whose comments and insights helped significantly improve the paper. We would also like thank the editors of Sedimentologika, particularly Murray Gingras, who worked diligently to shepherd this paper through the long process to publication. Silhouette images downloaded from Phylopic are by Beth Reinke (*Rana sierrae*), Edwin Price (*Chrysemys picta*), Ferran Sayol (*Alligator missisipensis*, *Leioheterodon madagascariensis*), Ingo Braasch (*Lepisosteus oculatus*), Jagged Fang Designs (*Jinzhousaurus yangi*), Guillame Dera (*Metanephrops japonicus*), and Zimices (*Strophodus rebecae*) and used under a CC0 1.0 Universal license. To view a copy of this license, visit http://creativecommons.org/publicdomain/zero/1.0. Research was funded in part by the State of Texas Advanced Resource Recovery Program at the Bureau of Economic Geology, University of Texas at Austin, the National Geographic Society Conservation Trust Grant C325-16, and an Experiment.com crowdfunding campaign.

Author contribution

Christopher Noto designed the research and sampled the Arlington Archosaur section. Peter Flaig did the sedimentological study of the outcrop, and Maria A. Lorente did the palynological analyses. All authors contributed equally to the results analysis and the manuscript's writing.

Data availability

The original data referenced in this paper can be accessed at the following free repository bioRxiv (Lorente et al., 2023): https://doi.org/10.1101/2023.12.04.569281.

Conflict of interest

The authors have no conflicts of interest to declare.

References

Abbink, O., Van Konijnenburg-Van Cittert, J., & Visscher, H. (2004). A sporomorph ecogroup model for the Northwest European Jurassic - Lower Cretaceous: Concepts and framework. Netherlands Journal of Geosciences, 83(1), 17-31. https://doi.org/10.1017/S0016774600020436

Adams, R. L., & Carr, J. P. (2010). Regional depositional systems of the Woodbine, Eagle Ford, and Tuscaloosa of the US Gulf Coast. Gulf Coast Association of Geological Societies Transactions, 60, 3-27. https://archives.datapages.com/data/gcags_pdf/2010/Papers/adamcarr.htm

Adams, T. L., Polcyn, M. J., Mateus, O., Winkler, D. A., & Jacobs, L. L. (2011). First occurrence of the long-snouted crocodyliform Terminonaris (Pholidosauridae) from the Woodbine Formation (Cenomanian) of Texas. Journal of Vertebrate Paleontology, 31(3), 712-716. https://doi.org/10.1080/02724634.2011.572938

Adams, T. L., Noto, C. R., & Drumheller, S. K. (2017). A large neosuchian crocodyliform from the Upper Cretaceous (Cenomanian) Woodbine Formation of North Texas. Journal of Vertebrate Paleontology, e1349776. https://doi.org/10.1080/02724634.2017.1349776

Adams, T., Drumheller, S., & Noto, C. R. (2023). Palaeodiversity and niche partitioning of crocodylomorphs from the Woodbine Group (Late Cretaceous; Cenomanian). In Yuong-Nam Lee (Ed.). Windows into Sauropsid and Synapsid Evolution: Essays in honor of Prof. Louis L. Jacobs (pp. 99-119). Dinosaur Science Center Press, South Korea.

Adrian, B., Smith, H., Noto, C. R., & Grossman, A. (2019). A new baenid, "Trinitichelys" maini sp. nov., and other fossil turtles from the Upper Cretaceous Arlington Archosaur Site (Woodbine Formation, Cenomanian), Texas, U.S.A. Palaeontologia Electronica, 22.3.81. https://doi.org/10.26879/1001

Adrian, B., Smith, H., Noto, C. R., & Grossman, A. (2021). An early bothremydid from the Arlington Archosaur Site of Texas. Scientific Reports, 11(9555). https://doi.org/10.1038/s41598-021-88905-1

Adrian, B., Smith, H., & Noto, C. R. (2023). A revision of "Trinitichelys" maini (Testudines: Baenidae) and additional material of its new genus from the Lewisville Formation (Woodbine Group, Cenomanian), Texas, USA. Palaeontologia Electronica, 26.2.a28. https://doi.org/10.26879/1266

Ambrose, W. E., Hentz, T. F., Bonnaffé, F., Loucks, R. G., Brown Jr., L. F., Wang, F.P., & Potter, E. (2009) Sequence-stratigraphic controls on complex reservoir architecture of highstand fluvial-dominated deltaic and lowstand valley-fill deposits in the Upper Cretaceous (Cenomanian) Woodbine Group, East Texas field: Regional and local perspectives. American Association of Petroleum Geologists Bulletin, 93 (2), 231-269. https://doi.org/10.1306/09180808053

Andrzejewski, K., & Tabor, N. J. (2020). Paleoenvironmental and paleoclimatic reconstruction of Cretaceous (Aptian-Cenomanian) terrestrial formations of Texas and Oklahoma using phyllosilicates. Palaeogeography, Palaeoclimatology, Palaeoecology, 543, 109491. htpps://doi.org/10.1016/j.palaeo.2019.109491

Barron, A.P. (2015). Palynological Interpretations of Deep Sea Drilling Projects Cores in the Gulf of Mexico and Bahamian Platform [Master's thesis, Missouri University of Science and Technology]. Masters Theses, 7387. https://scholarsmine.mst.edu/masters_theses/7387

Benson, R. B., Mannion, P. D., Butler, R. J., Upchurch, P., Goswami, A., & Evans, S. E. (2013). Cretaceous tetrapod fossil record sampling and faunal turnover: implications for biogeography and the rise of modern clades. Palaeogeography, Palaeoclimatology, Palaeoecology, 372, 88-107. https://doi.org/10.1016/j.palaeo.2012.10.028

Bergquist, H. R. (1949). Geology of the Woodbine formation of Cooke, Grayson, and Fannin Counties, Texas. Oil and Gas Investigation Map OM-98, U. S. Geological Survey. https://doi.org/10.3133/om98

Behrensmeyer, A. K., Kidwell, S. M., & Gastaldo, R. A. (2000). Taphonomy and paleobiology. Paleobiology, 26(S4), 103-147. https://www.jstor.org/stable/pdf/1571655.pdf

Brinkhuis, H. (1994). Late Eocene to Early Oligocene dinoflagellate cysts from the Priabonian type-area (northeast Italy): biostratigraphy and paleoenvironmental interpretation. Palaeogeography, Palaeoclimatology, Palaeoecology, 107(1-2), 121-163. https://doi.org/10.1016/0031-0182(94)90168-6

Brown C. W., & Pierce, R. L. (1962). Palynologic correlations in Cretaceous Eagle Ford group, northeast Texas. Bulletin of the American Association of Petroleum Geologists, 46(12), 2133-2147. https://doi.org/10.1306/BC743957-16BE-11D7-8645000102C1865D

Buatois, L. A., Gingras, M. K., MacEachern, J., Mángano, M. G., Zonneveld, J. P., Pemberton, S. G., Netto, R. G., & Martin, A. (2005). Colonization of brackish-water systems through time: Evidence from the trace-fossil record. PALAIOS, 20(4), 321-347. https://doi.org/10.2110/palo.2004.p04-32

Buntin, R. C. C., Hasiotis, S. T., & Flaig, P. P. (2022). Evaluating the ichnofossil Teredolites as an indicator of salinity and paleoenvironment. PALAIOS, 37(3), 53-72. https://doi.org/10.2110/palo.2020.074

Catuneanu, O. (2006). Principles of Sequence Stratigraphy. Developments in sedimentology, 58, Elsevier, Amsterdam, 375 p. ISBN 978-0-444-53353-1

Cavin, L., Toriño, P., Van Vranken, N., Carter, B., Polcyn, M. J., & Winkler, D. (2021). The first late cretaceous mawsoniid coelacanth (Sarcopterygii: Actinistia) from North America: Evidence of a lineage of extinct 'living fossils'. PLoS One, 16(11), e0259292. https://doi.org/10.1371/journal.pone.0259292

Chowdhury, K. R. (1982). Distribution of Recent and fossil palynomorphs in the south eastern North Sea. Senckenbergiana Maritima, 14(3-4), 79-145.

Christopher, R. A. (1979). Normapolles and triporate pollen assemblages from the Raritan and Magothy formations (Upper Cretaceous) of New Jersey. Palynology, 3(1), 73-122. https://doi.org/10.1080/01916122.1979.9989185

Christopher, R. A. (1982). The occurrence of the Complexiopollis–Atlanopollis zone (Palynomorphs) in the Eagle Ford Group (Upper Cretaceous) of Texas. Journal of Paleontology, 56(2), 525-541. https://www.jstor.org/stable/1304481

Cloos, M. (2018). Palynology of the Cenomanian Woodbine Group [Master's thesis, Southern Methodist University]. Earth Sciences Theses and Dissertations, 8. https://scholar.smu.edu/hum_sci_earthsciences_etds/8

Cobban, W. A., Walaszczyk, I., Obradovich, J. D., & McKinney, K. C. (2006). A USGS zonal table for the Upper Cretaceous middle Cenomanian–Maastrichtian of the Western Interior of the United States based on ammonites, inoceramids, and radiometric ages (Open-File Report 2006-1250). United States Geological Survey. https://pubs.usgs.gov/of/2006/1250/

Denne, R. A., & Breyer, J. A. (2016). Regional depositional episodes of the Cenomanian-Turonian Eagle Ford and Woodbine groups of Texas and their relationship to Oceanic Anoxic Event

2 (OAE2). Gulf Coast Association of Geological Societies Transactions, 66, 145-158. https://shorturl.at/fiARZ

Denne, R. A., Breyer, J. A., Kosanke, T. H., Spaw, J. M., Callender, A. D., Hinote, R. E., Kariminia, M., Tur, N., Kita, Z., Lees, J.A. & Rowe, H. (2016). Part 1: Biostratigraphic and geochemical constraints on the stratigraphy and depositional environments of the Eagle Ford and Woodbine Groups of Texas. In J. A. Breyer (Ed.). The Eagle Ford Shale: A renaissance in U.S. oil production, AAPG Memoir 110, 1-86. https://doi.org/10.1306/13541957M1103660

Dodge, C. F. (1952). Stratigraphy of the Woodbine Formation in the Arlington area. Tarrant County, Texas. Field and Laboratory, 20, 66–78.

Dodge, C. F. (1968). Stratigraphic nomenclature of the Woodbine Formation Tarrant County, Texas. In Dodge, C. F (Ed.). Field trip Guidebook, South Central Section, Stratigraphy of the Woodbine Formation, Tarrant County, Texas. Colorado (pp. 107-125). Geological Society of America.

Dodge, C. F. (1969). Stratigraphic nomenclature of the Woodbine Formation Tarrant County, Texas. Texas Journal of Science, 21, 43-62.

Dodsworth, P. (2016). Palynostratigraphy and Palaeoenvironments of the Eagle Ford Group (Upper Cretaceous) at the Lozier Canyon Outcrop Reference Section, West Texas, USA. Palynology, 40(3), 357-378. https://doi.org/10.1080/01916122.2015.1073188

Dodsworth, P., & Eldrett, J. S. (2019). A dinoflagellate cyst zonation of the Cenomanian and Turonian (Upper Cretaceous) in the Western Interior, United States. Palynology, 43(4), 701-723. https://doi.org/10.1080/01916122.2018.1477851

Donovan, A.T., Staerker, S., Gardner, R., Pope, M., Pramudito, A., & Wehner, M. (2016). Findings from the Eagle Ford outcrops of west Texas and implications to the subsurface of south Texas. In J. A. Breyer (Ed.). The Eagle Ford Shale: A renaissance in U.S. oil production, AAPG Memoir 110, 301-336. https://doi.org/10.1306/13541967M1101083

Drumheller, S. K., Adams, T. L., Maddox, H., & Noto, C. R. (2021). Expanded sampling across ontogeny in Deltasuchus motherali (Neosuchia, Crocodyliformes) reveals ecomorphological niche partitioning and Appalachian endemism in Cenomanian crocodyliforms. Cambridge Elements of Paleontology, 92. https://doi.org/10.1017/9781009042024

Dupont, L.M., & Agwu, C.O.C. (1991) Environmental control of pollen grain distribution patterns in the Gulf of Guinea and offshore NW-Africa. Geologische Rundschau, 80, 567-589. https://doi.org/10.1007/BF01803687

Eaton, J. G. (1999). Vertebrate paleontology of the Iron Springs Formation, Upper Cretaceous, southwestern Utah. In Gillette, D. D. (Ed.). Vertebrate paleontology in Utah (pp. 339-343). Utah Geological Survey.

Eaton, J. G., Kirkland, J. I., Hutchison, J. H., Denton, R., O'Neill, R. C., & Parrish, J. M. (1997). Nonmarine extinction across the Cenomanian-Turonian boundary, southwestern Utah, with a comparison to the Cretaceous-Tertiary extinction event. Geological Society of America Bulletin, 109(5), 560-567. https://shorturl.at/hlNQ2

Eldrett, J. S., Minisini, D., & Bergman, S. C. (2014). Decoupling of the carbon cycle during Ocean Anoxic Event 2. Geology, 42(7), 567–570. https://doi.org/10.1130/G35520.1

Eldrett, J. S., Ma, C., Bergman, S. C., Lutz, B., Gregory, F. J., Dodsworth, P., Phipps, M., Hardas, P., Minisini, D., Ozkan, A., & Ramezani, J. (2015a). An astronomically calibrated stratigraphy of the Cenomanian, Turonian and earliest Coniacian from the Cretaceous Western Interior Seaway, USA: Implications for global chronostratigraphy. Cretaceous Research, 56, 316-344. https://doi.org/10.1016/j.cretres.2015.04.010

Eldrett J. S., Dodsworth, P., Bergman, S., Wright, M., & Minisini, D. (2017). Water-mass evolution in the Cretaceous Western Interior Seaway of North America and equatorial Atlantic. Climate of the Past, 13(7), 855-878. https://doi.org/10.5194/cp-13-855-2017

Farley, M. B., & Dilcher, D. L. (1986). Correlation between miospores and depositional environments of the Dakota Formation (Mid-Cretaceous) of North Central Kansas and adjacent Nebraska, USA. Palynology, 10(1), 117-133. https://doi.org/10.1080/01916122.1986.9989306

Falzoni, F., & Petrizzo, M. R. (2022). Evidence for changes in sea-surface circulation patterns and ~20° equatorward expansion of the Boreal bioprovince during a cold snap of Oceanic Anoxic Event 2 (Late Cretaceous). Global and Planetary Change, 208, 103678. https://doi.org/10.1016/j.gloplacha.2021.103678

Fan, D. D., & Li, C. X. (2002). Rhythmic deposition on mudflats in the mesotidal Changjiang estuary, China. Journal of Sedimentary Research, 72(4), 543-551. https://doi.org/10.1306/112901720543

Flaig, P. P., McCarthy, P. J., & Fiorillo, A. R. (2011). A tidally influenced, high-latitude coastal-plain: the Upper Cretaceous (Maastrichtian) Prince Creek Formation, North Slope, Alaska. In Davidson, S., Leleu, S., & North, C. (Eds.). From River to Rock Record: The Preservation of Fluvial Sediments and Their Subsequent Interpretation (pp. 233-264). SEPM Special Publication 97. https://doi.org/10.2110/sepmsp.097.233

Flaig, P. P., McCarthy, P. J., & Fiorillo, A. R. (2013). Anatomy, evolution, and paleoenvironmental interpretation of an ancient arctic coastal plain: Integrated paleopedology and palynology from the upper Cretaceous (Maastrichtian) Prince Creek Formation, North Slope, Alaska, USA. In Driese, S. G., & Nordt, L. C. (Eds.). New Frontiers in Paleopedology and Terrestrial Paleoclimatology, Paleosols and Soil Surface Analogue Systems (pp. 179-230). SEPM Special Publication 114. https://doi.org/10.2110/sepmsp.104

Flaig, P. P., Hasiotis, S. T., Prather, T. J., & Burton, D. (2019). Characteristics of a Campanian delta deposit controlled by alternating river-floods and tides: The Loyd Sandstone, Rangely Anticline, Colorado, U.S.A. Journal of Sedimentary Research, 89(12), 1181-1206. https://doi.org/10.2110/jsr.2019.63

Flaig, P. P., Denison, C. N., Ambrose, W. A., & Demchuk, T. D. (2022). Outcrop evidence for variations in channel-floodplain facies and stratal architectures across the Simsboro to Calvert Bluff transition, Wilcox Group, Butler, Texas. GCAGS Journal, 11, 83-103. https://shorturl.at/bmQU2

Gifford, S. R. (2021). The Sequence Stratigraphy of the Woodbine and Eagle Ford Groups in the East Texas Basin (USA): A new Chronostratigraphic Framework to Properly Identify & Map their Associated Plays and Play Fairways [Master's thesis, Texas A&M University]. Oaktrust–Texas A&M University Library. https://hdl.handle.net /1969.1/193195

Gradstein, F.M., Ogg, J.G., Schmitz, M.D., & Ogg, G.M. (Eds.). (2012). The Geologic Time Scale 2012. Elsevier. https://doi.org/10.1016/C2011-1-08249-8

Hacker, R. J., & Shimada, K. (2021). A new ichthyodectiform fish (Actinopterygii: Teleostei) from the Arlington Member (mid-Cenomanian) of the Upper Cretaceous Woodbine Formation in Texas, USA. Cretaceous Research, 123, 104798. https://doi.org/10.1016/j.cretres.2021.104798

Harris, A. J., & Tocher, B. A. (2003). Palaeoenvironmental analysis of Late Cretaceous dinoflagellate cyst assemblages using high-resolution sample correlation from the Western Interior Basin, USA. Marine Micropaleontology, 48(1-2), 127-148. https://doi.org/10.1016/S0377-8398(03)00002-1

Head, J. J. (1998). A new species of basal hadrosaurid (Dinosauria, Ornithischia) from the Cenomanian of Texas. Journal of Vertebrate Paleontology, 18(4), 718-738. https://www.jstor.org/stable/4523950

Hedlund, R.W. (1966). Palynology of the Red Branch Member of the Woodbine Formation, (Cenomanian), Bryan County, Oklahoma (Bulletin 112, pp.1-69). Oklahoma Geological Survey, Norman. http://www.ogs.ou.edu/pubsscanned/BULLETINS/Bulletin112.pdf

Heimhofer, U., Wucherpfennig, N., Adatte, T., Schouten, S., Schneebeli-Hermann, E., Gardin, S., Keller, G., Kentsch, S., & Kujau, A. (2018). Vegetation response to exceptional global warmth during Oceanic Anoxic Event 2. Nature Communications, 9, 3832. https://doi.org/10.1038/s41467-018-06319-6

Hentz, T. F., Ambrose, W. A., & Smith, D. C. (2014). Eaglebine play of the southwestern East Texas basin: Stratigraphic and depositional framework of the Upper Cretaceous (Cenomanian–Turonian) Woodbine and Eagle Ford Groups. AAPG Bulletin, 98(12), 2551–2580. https://doi.org/10.1306/07071413232

Heusser, L. E., & Balsam, W. L. (1977). Pollen distribution in the northeast Pacific Ocean. Quaternary Research, 7(1), 45-62. https://doi.org/10.1016/0033-5894(77)90013-8

Heusser, L. E. (1985). Quaternary palynology of marine sediments in the northeast Pacific, northwest Atlantic, and Gulf of Mexico. In V. M. Bryant Jr & R. G. Holloway (Eds.). Pollen Records of Late Quaternary North American Sediments (pp. 385-404). American Association of Stratigraphic Palynologists Foundation.

Heusser, L. E., & Balsam, W. L. (1985). Pollen sedimentation in the northwest Atlantic: effects of the Western Boundary Undercurrent. Marine Geology, 69(1-2), 149-153. https://doi.org/10.1016/0025-3227(85)90138-0

Heusser, L. E. (1988). Pollen distribution in marine sediments on the continental margin off northern California. Marine Geology, 80(1-2), 131-147. https://doi.org/10.1016/0025-3227(88)90076-X

Jacobs, L. L., & Winkler, D. A. (1998). Mammals, archosaurs, and the Early to Late Cretaceous transition in north-central Texas. In Y. Tomida, L. J. Flynn, & L. L. Jacobs (Eds.). Advances in Vertebrate Paleontology and Geochronology (pp. 253-280). National Science Museum Monographs 14. https://cir.nii.ac.jp/crid/1571417126926663680

Jacobs, L. L., Ferguson, K., Polcyn, M. J., & Rennison, C. (2005). Cretaceous $\delta^{13}C$ stratigraphy and the age of dolichosaurs and early mosasaurs. Netherlands Journal of Geosciences, 84(3), 257-268. https://doi.org/10.1017/S0016774600021041

Johnson, R. O. (1974). Lithofacies and depositional environments of the Rush Creek Member of the Woodbine Formation (Gulfian) of North Central Texas [Master's thesis, University of Texas].

Kennedy, W. J., & Cobban, W. A. (1990). Cenomanian ammonite faunas from the Woodbine Formation and lower part of the Eagle Ford Group, Texas. Palaeontology, 33(1), 75-154. http://go.palass.org/4gh

Krause, D. W., & Baird, D. (1979). Late Cretaceous mammals east of the North American western interior seaway. Journal of Paleontology, 562-565. https://www.jstor.org/stable/1303997

Lee, Y.-N. (1997). The Archosauria from the Woodbine Formation (Cenomanian) in Texas. Journal of Paleontology, 71(6), 1147-1156. https://doi.org/10.1017/S0022336000036088

Lorente, M. A. (1986). Palynology and palynofacies of the Upper Tertiary in Venezuela [Ph.D dissertation]. Dissertationes Botanicae, Band 99. Lubrecht & Cramer Ltd., Port Jervis.

Lorente, M. A. (1990). Textural characteristics of organic matter in several subenvironments of the Orinoco upper delta. Geologie en Mijnbouw, 69, 263-278. http://pascal-francis.inist.fr/vibad/index.php?action=getRecordDetail&idt=6901731

Lorente, M. A., Noto, C. R., & Flaig, P. (2023). A Glimpse into the Cenomanian: Palynology of the Arlington Archosaur Site, Late Cretaceous Western Interior Seaway, Texas, USA. bioRxiv, 2023.12.04.569281. https://doi.org/10.1101/2023.12.04.569281

MacEachern, J. A., & Bann, K. L. (2008). The role of ichnology in refining shallow marine facies models. In G. J. Hampson, R. J. Steel, P. M. Burgess, & R. W. Dalrymple (Eds.). Recent advances in models of siliciclastic shallow-marine stratigraphy (pp. 73-116). SEPM Special Publication 90. https://doi.org/10.2110/pec.08.90.0073

Main, D. J. (2013). Appalachian Delta Plain Paleoecology of the Cretaceous Woodbine Formation at the Arlington Archosaur Site North Texas [Ph.D. Dissertation, The University of Texas at Arlington]. ResearchCommons, UTA Libraries. http://hdl.handle.net/10106/11888

Main, D. J., Noto, C. R., & Weishampel, D. B. (2014). Postcranial anatomy of a basal hadrosauroid (Dinosauria: Ornithopoda) from the Cretaceous (Cenomanian) Woodbine Formation of North Central Texas. In D. Eberth & D. Evans (Eds.). Hadrosaurs (pp. 77-95). Indiana University Press.

Martin, R. E. (1999). Taphonomy: a process approach. https://doi.org/10.1017/CBO9780511612381

McNulty Jr, C. L., & Slaughter, B. H. (1962). A new sawfish from the Woodbine Formation (Cretaceous) of Texas. Copeia, 775-777. https://www.jstor.org/stable/1440678

McNulty, C. L., & Slaughter, B. H. (1968). Fishbed conglomerate fauna, Arlington Member, Woodbine Formation (Cenomanian) of Texas. In Dodge, C. F. (Ed.). Stratigraphy of the Woodbine Formation: Tarrant County, Texas Field Trip Guidebook (pp. 68-73). Geological Society of America, South Central Section.

Mudie, P. J. (1982). Pollen distribution in Recent marine sediments, eastern Canada. Canadian Journal of Earth Sciences, 19(4), 729-747. https://doi.org/10.1139/e82-062

Muller, J. (1959). Palynology of Recent Orinoco Delta and shelf sediments: reports of the Orinoco Shelf expedition; volume 5. Micropaleontology, 5(1), 1-32. https://doi.org/10.2307/1484153

Nesbitt, S. J., Denton, R. K., Loewen, M. A., Brusatte, S. L., Smith, N. D., Turner, A. H., Kirkland, J. I., McDonald, A. T., & Wolfe, D. G. (2019). A mid-Cretaceous tyrannosauroid and the origin of North American end-Cretaceous dinosaur assemblages. Nature Ecology & Evolution, 3(6), 892-899. https://doi.org/10.1038/s41559-019-0888-0

Norstog, K. J. (2023, May 9). Cycad. Encyclopedia Britannica. https://www.britannica.com/plant/cycad.

Noto, C. R. (2015). Archosaur Localities in the Woodbine Formation (Cenomanian) of North-Central Texas. In C. Noto (Ed.). Early- and Mid-Cretaceous Archosaur Localities of North-Central Texas, Fieldtrip Guidebook for the 75th Annual Meeting of the Society of Vertebrate Paleontology, Dallas, Texas (pp. 38-51). https://doi.org/10.6084/m9.figshare.1608173.v1

Noto, C. R., Main, D. J., & Poole, K. (2013). Phylogenetic and biostratigraphic implications of new postcranial material of Protohadros (Ornithopoda, Hadrosauroidea) from the Woodbine Formation of Texas. Journal of Vertebrate Paleontology, Program and Abstracts, 33, 185. https://vertpaleo.org/svp-2013-merged-book-10-15-2013/

Noto, C. R., Adams, T. L., Drumheller, S. K., & Turner, A. H. (2019). A small enigmatic neosuchian crocodyliform from the Woodbine Formation of Texas. The Anatomical Record, 303(4), 801-812. https://doi.org/10.1002/ar.24174

Noto, C. R., D'Amore, D., Drumheller, S., & Adams, T. (2022). A newly recognized theropod assemblage from the Lewisville Formation (Woodbine Group; Cenomanian) and its implications for understanding Late Cretaceous Appalachian terrestrial ecosystems. PeerJ, 10, e12782. https://doi.org/10.7717/peerj.12782

Noto, C., Flaig, P., Contreras, D., Zippi, P., Lorente, M., Andrzejewski, K., & Tykoski, R. (2023a). Deciphering the Woodbine Group (Late Cretaceous; Cenomanian) outcrops of the Dallas–Ft. Worth Metroplex: new data and new horizons. 14th Symposium on Mesozoic Terrestrial Ecosystems and Biota. The Anatomical Record, 306(S1), 206-208. https://doi.org/10.1002/ar.25219

Noto, C., Drumheller, S., Adams, T., Adrian, B., Smith, H., Tykoski, R., & Flaig, P. (2023b). Faunal composition, distribution, and paleobiogeography of fossil vertebrates from the Lewisville Formation (Woodbine Group, Cenomanian). 14th Symposium on Mesozoic Terrestrial Ecosystems and Biota. The Anatomical Record, 306(S1), 203-206. https://doi.org/10.1002/ar.25219

Ogg, J. G., & Hinnov, L. A., (2012). The Cretaceous Period. In Gradstein, F.M., Ogg, J.G., Schmitz, M.D., & Ogg, G.M. (Eds.). The Geologic Time Scale 2012. Elsevier. https://doi.org/10.1016/B978-0-444-59425-9.00027-5

Olariu, C., Bhattacharya, J. P., Xu, X., Aiken, C. L. V., Zeng, X., & McMechan, G.A. (2005). Integrated study of ancient delta front deposits, using outcrop, ground penetrating radar, and three dimension photorealistic data: Cretaceous Panther Tongue sandstone, Utah. In L. Giosan & J. P. Bhattacharya (Eds.). River Deltas: Concepts, Models, and Examples (pp. 155–177). SEPM Special Publication 83. https://doi.org/10.2110/pec.05.83.0155

Olariu, C., & Bhattacharya, J.P. (2006). Terminal distributary channels and delta front architecture of river-dominated delta systems. Journal of Sedimentary Research, 76(2), 212–233. https://doi.org/10.2110/jsr.2006.026

Olde, K., Jarvis, I., Ulicnỳ, D., Pearce, M., Trabucho-Alexandre,J., Cech, S., Grocke, D., Laurin, J., Svabenicka, L., & Tocher, B. (2015). Geochemical and palynological sea-level proxies in hemipelagic sediments: a critical assessment from the Upper Cretaceous of the Czech Republic. Palaeogeography, Palaeoclimatology, Palaeocology, 435, 222-243. https://doi.org/10.1016/j.palaeo.2015.06.018

Oliver, W. (1971). Depositional Systems in Woodbine Formation (Upper Cretaceous), Northeast Texas. AAPG Bulletin, 55(1), 156-156. https://doi.org/10.23867/RI0073D

Ostrowski, S. A., & Noto, C. R. (2017). Hold me closer tiny fossil: a rich microvertebrate fauna from the Arlington Archosaur Site (Woodbine Formation, Cenomanian) of north-central Texas. Journal of Vertebrate Paleontology, Program and Abstracts, 173. https://vertpaleo.org/svp-2017-program-book-v6-print-ready-with-front-cover/

Ostrowski, S. A., & Noto, C. R. (2023). Have your snake and eat it too: snake material from the Arlington Archosaur Site (Lewisville Formation, Cenomanian) of north-central Texas. 14th Symposium on Mesozoic Terrestrial Ecosystems and Biota. The Anatomical Record, 306(S1), 210-211. https://doi.org/10.1002/ar.25219

Pérez-García, A., Bardet, N., Fregenal-Martínez, M. A., Martín-Jiménez, M., Mocho, P., Narváez, I., Torices, A., Vullo, R., & Ortega, F. (2020). Cenomanian vertebrates from Algora (central Spain): New data on the establishment of the European Upper Cretaceous continental faunas. Cretaceous Research, 115, 104566. https://doi.org/10.1016/j.cretres.2020.104566

Poumot, C. (1989). Palynological evidence for eustatic events in the tropical Neogene. Bulletin des Centres de Recherches Exploration-Production Elf Aquitaine, 13(2), 437-453. http://pascal-francis.inist.fr/vibad/index.php?action=getRecordDetail&idt=6632083

Powell, J. D. (1968). Woodbine-Eagle Ford transition, Tarrant Member. In Dodge, C. F. (Ed.). Stratigraphy of the Woodbine Formation: Tarrant County, Texas Field Trip Guidebook (pp. 27-43). Geological Society of America, South Central Section.

Retallack, G. J. (2001). Soils of the Past (2nd ed.). Blackwell Science. https://onlinelibrary.wiley.com/doi/book/10.1002/9780470698716

Scott, R. W., Holbrook J. M., Oboh-Ikuenobe, F., Evetts M. J., Benson, D. G., & Kues, B. S. (2004). Middle Cretaceous Stratigraphy, Southern Western Interior Seaway, New Mexico and Oklahoma. The Mountain Geologist, 41(2), 33-61. https://archives.datapages.com/data/rmag/mg/2004/scott.htm

Sellards, E. H., Adkins, W. S., & Plummer F. B. (1932). The Geology of Texas Vol.1, Stratigraphy (Bulletin 3232). University of Texas, Austin.

Slattery, J. S., Cobban, W. A., McKinney, K. C., Harries, P. J., & Sandness, A. L. (2015). Early Cretaceous to Paleocene paleogeography of the Western Interior Seaway: the interaction of eustasy and tectonism. In M. Bingle-Davis (Ed.). Wyoming Geological Association 15th Annual Field Conference Guidebook (pp. 22-60). Casper, Wyoming. https://shorturl.at/cqDEG

Sluijs, A., Pross, J., & Brinkhuis, H. (2005). From greenhouse to icehouse; organic-walled dinoflagellate cysts as paleoenvironmental indicators in the Paleogene. Earth-Science Reviews, 68(3–4), 281-315. https://doi.org/10.1016/j.earscirev.2004.06.001

Smith, V., Hessler, A., Moscardelli, L., Bord, D., Olariu, I., Lorente, M. A., Sivil, E., & Liu, X. (2024). A late refugium for Classopollis in the Paleocene Lower Wilcox Group along the Texas Gulf Coast. Geology, 52 (4), 251–255. https://doi.org/10.1130/G51772.1

Stephenson, L. W. (1952). Larger Invertebrate Fossils of the Woodbine Formation (Cenomanian) of Texas. USGS Professional Paper, 242, 1-211. https://doi.org/10.3133/pp242

Tschudy, R. H. (1969). Relationship of palynomorphs to sedimentation. In R. H. Tschudy & R. A. Scott (Eds.). Aspects of Palynology (pp. 79-96). Wiley. https://search.worldcat.org/title/aspects-of-palynology/oclc/51371

Trudel, P. (1994). Stratigraphic sequences and facies architecture of the Woodbine–Eagle Ford interval, Upper Cretaceous, North Central Texas [Unpublished Master's thesis]. Tarleton State University.

Tucker, R. T., Zanno, L. E., Huang, H. Q., & Makovicky, P. J. (2020). A refined temporal framework for newly discovered fossil assemblages of the upper Cedar Mountain Formation (Mussentuchit Member), Mussentuchit Wash, Central Utah. Cretaceous Research, 110, 104384. https://doi.org/10.1016/j.cretres.2020.104384

Tucker, R. T., King, M. R., Mohr, M. T., Renaut, R. K., Crowley, J. L., Fekete, J. W., Makovicky, P. J., & Zanno, L. E. (2024), Tectono-sedimentary history of the upper Cedar Mountain Formation, Central Utah, USA. Sedimentology. https://doi.org/10.1111/sed.13211

Tykoski, R. S., & Fiorillo, A. R. (2010). An enantiornithine bird from the lower middle Cenomanian of Texas. Journal of Vertebrate Paleontology, 30(1), 288-292. https://doi.org/10.1080/02724630903416068

UCMP, University of California Museum of Paleontology. (n.d.). Introduction to the Cycads. Legacy of the Mesozoic. https://ucmp.berkeley.edu/seedplants/cycadophyta/cycads.html

Vallabhaneni, S., Olszewski, T.D., Pope, M. C., & Heidari, Z. (2016). Facies and stratigraphic interpretation of the Eaglebine Play in Central Texas. GCAGS Journal, 5, 25-46. https://shorturl.at/yGJU0

van der Kolk, D. A., Flaig, P. P., & Hasiotis, S. T. (2015). Paleoenvironmental reconstruction of a Late Cretaceous, muddy, river-dominated polar deltaic system: Schrader Bluff - Prince Creek Formation transition, Shivugak Bluffs, North Slope of Alaska, U.S.A. Journal of Sedimentary Research, 85(8), 903–936. http://doi.org/10.2110/jsr.2015.58

van Helmond N. A. G. M., Sluijs, A., Papadomanolaki, N. M., Plint, G., Gröcke, D. R., Pearce, M. A., Eldrett, J. S., Trabucho-Alexandre, J., Walaszczyk, I., van de Schootbrugge, B., & Brinkhuis, H. (2016). Equatorward phytoplankton migration during a cold spell within the Late Cretaceous super-greenhouse. Biogeosciences, 13(9), 2859-2872. https://doi.org/10.5194/bg-13-2859-2016, 2016

Wall, D., Dale, B., Lohmann, G. P., & Smith, W. K. (1977). The environment and climatic distribution of dinoflagellate cysts in modem marine sediments from regions in the North and South Atlantic Oceans and adjacent seas. Marine Micropalaeontology, 2, 121-200. https://doi.org/10.1016/0377-8398(77)90008-1

Williams, D. B., & Sarjeant, W. A. S. (1967). Organic-walled microfossils as depth and shoreline indicators. Marine Geology, 5(5–6), 389-412. https://doi.org/10.1016/0025-3227(67)90050-3

Zanno, L. E., & Makovicky, P. J. (2013). Neovenatorid theropods are apex predators in the Late Cretaceous of North America. Nature Communications, 4(1), 2827. https://doi.org/10.1038/ncomms3827

How to cite: Noto, C. R., Flaig, P. P., & Lorente, M. A. (2025). Multiproxy synthesis at the Arlington Archosaur Site: New insights into Cretaceous paralic paleoenvironments and regional stratigraphy, Woodbine Group, Texas, USA. Sedimentologika, 3(1), 1-24. https://doi.org/10.57035/journals/sdk.2025.e31.1435